Nat. Hazards Earth Syst. Sci. Discuss., doi:10.5194/nhess-2017-75, 2017
Manuscript under review for journal Nat. Hazards Earth Syst. Sci.
Discussion started: 4 May 2017

Natural Hazards and Earth System Sciences
Discussions

Tsunami evacuation plans for future megathrust earthquakes in Padang, Indonesia considering stochastic earthquake scenarios

Ario Muhammad[1,2], Katsuichiro Goda[1], Nicholas A. Alexander[1], Widjo Kongko[3], and Abdul Muhari[4]

[1]Department of Civil Engineering, University of Bristol, Bristol, BS8 1TR, UK
[2]Department of Civil Engineering, University of Narotama, Surabaya, 60117, Indonesia
[3]Agency for the Assessment & Application of Technology (BPPT), Yogyakarta, 55281, Indonesia
[4]Directorate General for Marine Spatial Management, Ministry of Marine Affairs and Fisheries, Jakarta, 10110, Indonesia

Correspondence to: Ario Muhammad (ario.muhammad@bristol.ac.uk)

Abstract. This study develops tsunami evacuation plans in Padang, Indonesia, using a stochastic tsunami simulation method. The stochastic results are based on multiple earthquake scenarios for different magnitudes (Mw 8.5, 8.75, and 9.0) that reflect asperity characteristics of the 1797 historical event in the same region. The generation of the earthquake scenarios involves probabilistic models of earthquake source parameters and stochastic synthesis of earthquake slip distributions. In total, 300 source models are generated to produce comprehensive tsunami evacuation plans in Padang. The tsunami hazard assessment results show that Padang may face significant tsunamis causing the maximum tsunami inundation height and depth of 15 m and 10 m, respectively. A comprehensive tsunami evacuation plan, including horizontal evacuation area maps, assessment of temporary tsunami evacuation shelters, and integrated horizontal-vertical evacuation time maps, has been developed based on the stochastic tsunami simulation results. The evacuation plans highlight that comprehensive mitigation policies can be produced from the stochastic tsunami simulation against the future tsunamigenic events.

1 Introduction

Tsunami hazard and risk assessments have become an important issue in tsunami-prone regions especially after the 2004 Aceh-Andaman earthquake (M_w 9.15) and the 2011 Tohoku earthquake (M_w 9.0). Significant risk mitigation efforts have been made in recent years in high-risk countries, such as Japan, U.S.A., Chile, New Zealand, and Indonesia (Schlurmann et al., 2010; Wood et al., 2014; Mueller et al., 2015; Raby et al., 2015). Despite the fact that Japan is a well-developed country with comprehensive tsunami defense systems, the 2011 Tohoku tsunami still caused significant damage claiming economic loss of ~365 billion USD and fatalities of ~20,000 people (Kazama and Noda, 2012). Globally, preparedness systems against the earthquake and tsunami hazards need to be improved to reduce the economic and social impact due to future tsunamigenic earthquake events (Scheer et al., 2011; Wood et al., 2012). Among the tsunami-prone countries, Indonesia is located in one of the most seismically active zones; there were 34 major tsunamigenic events in the last 20 years (USGS, 2015). In particular, past paleo-geodetic, paleo-tsunami, and geodetic investigations (e.g. Nalbant et al., 2005; Sieh et al., 2008) indicate that the Mentawai segment of the Sunda subduction zone (see FIGURE 1A) can host large tsunamigenic events (M_w > 8.5) with a

recurrence period of about 200 years. The last major tsunamigenic earthquakes in this region were the 1797 and 1833 events (Natawidjaja et al., 2006), while two recent events, M_w 8.4 and M_w 7.9, occurred near Bengkulu on 12 and 13 September 2007 (see FIGURE 1A). A study by Konca et al. (2007) concluded that the recent earthquakes released far smaller amounts of slip in comparison with the accumulated slip since 1833 and hence, the potential of a large tsunamigenic event originated from this source remains high.

Padang is the home of more than 850,000 and is one of the most urbanized cities in western Sumatra. It is located along the coast of Sumatra Island, directly facing the Mentawai segment of the Sunda subduction zone (see FIGURE 1A). Consequently, potential impact of the future tsunami may have significant risk in this area. In addition, with the low-lying plain topographic features in Padang, the probability of large inundated areas and large inundation depths is also high (Borrero et al., 2006; Muhari et al., 2010, 2011). In the past, two types of earthquake source scenarios have been mainly considered to develop tsunami risk mitigation plans in Padang: deterministic scenarios (Borrero et al., 2006; Schlurmann et al., 2010; Muhari et al., 2010, 2011) and probabilistic scenarios (McCloskey et al., 2008; Griffin et al., 2016). Implementation of deterministic scenarios may oversimplify the tsunami hazards and risks, leading to inaccurate mitigation plans (Mueller et al., 2014; Griffin et al., 2015). On the other hand, the probabilistic scenario approach requires the proper consideration of regional earthquake characteristics, including uncertainties in size of the rupture plane and spatial heterogeneity of earthquake slip; all of these factors have not been taken into account previously. Recently, Muhammad et al. (2016) have evaluated the tsunami potential in Padang by developing the stochastic tsunami simulation method allowing to generate numerous scenarios of stochastic tsunami hazard. However, that work was limited to evaluate the tsunami hazards off-shore and near coast only because of the gross bias of the elevation model in Padang (Griffin et al., 2015) and therefore, was not suitable to carry out rigorous assessment of tsunami mitigation systems. In addition, the gross bias of the elevation model in Padang is due to the use of global Digital Elevation Model (DEM; i.e. GDEM2) as the elevation data for the stochastic tsunami simulation. The absolute vertical errors of global DEM (e.g. GDEM2 and SRTM1) are in the range from 5 m to 10 m resulting in inaccurate prediction of the inundation footprints especially in coastal areas (Sanders, 2007; Gallegos, 2009; Lewis et al., 2013; Griffin et al., 2015). Thereby, this work also highlights the effect of DEM on inundation modeling in Padang areas which has not been studied in the previous investigations.

Moreover, an effective tsunami evacuation plan should combine both horizontal evacuation to high grounds and vertical evacuation to designated tsunami-resistant shelters (FEMA P-646, 2012). In the coastal areas where people can afford relatively short evacuation time (less than 30 minutes), the vertical evacuation is highly desirable (Scheer et al., 2012; Wood et al., 2014). In the previous investigations, the tsunami arrival time in Padang was estimated to be 20-30 minutes (Borrero et al., 2006; McCloskey et al., 2008; Schlurmann et al., 2010; Muhammad et al., 2016) and therefore, effective vertical evacuation plans are needed in this region. In Padang, 23 tsunami evacuation shelters (TES) have been planned and built in the urban areas near the coastal line. However, an extensive assessment of the TES in Padang during the tsunami event was not conducted by the previous studies (Schlurmann et al., 2010; Muhari et al., 2010, 2011; Imamura et al., 2011). Only horizontal evacuation time maps to safe areas were provided in Schlurmann et al. (2010) and hence, it is important to assess the TES in Padang as

Nat. Hazards Earth Syst. Sci. Discuss., doi:10.5194/nhess-2017-75, 2017
Manuscript under review for journal Nat. Hazards Earth Syst. Sci.
Discussion started: 4 May 2017

part of future tsunami mitigation planning. The results of the TES assessment can be further used to develop integrated horizontal-vertical tsunami evacuation maps.

Building upon the previous studies, this study develops tsunami evacuation plans in Padang based on the stochastic tsunami simulation method. This approach generates multiple earthquake scenarios by considering the uncertainties of the earthquake source parameters and slip distributions, both of which have major influence on the tsunami hazards. Hence, it is suitable to estimate the tsunami hazard level in Padang. Regional seismological characteristics are taken into account in generating stochastic earthquake scenarios based on the finite-fault models of the past earthquakes in the Sunda subduction zone. In addition, a 5-m high-resolution DEM of Padang (DEM5) developed by the German-Indonesian Tsunami Early Warning System (GITEWS) project and Indonesian research institutions is adopted as land elevation data for tsunami simulation. Combination of the stochastic tsunami inundation modeling and the high-resolution DEM significantly improves the accuracy of tsunami inundation modeling in Padang. Subsequently, the tsunami mitigation plans in Padang, i.e. tsunami inundation maps, TES assessments, and integrated horizontal-vertical evacuation time maps, are produced based on inundation depths estimated from the stochastic tsunami simulations. The development of such tsunami mitigation systems in Padang will overcome the limitations of the previous works and will contribute to improving the tsunami preparedness against the future catastrophic events.

2 Methodology

2.1. Tsunami modeling

2.1.1 Earthquake scenario selection

The stochastic tsunami simulation method (Muhammad et al., 2016) is adopted to estimate the tsunami hazard level in Padang. To generate earthquake source model stochastically, earthquake scenarios in terms of magnitude and source region need to be set up in advance. An appropriate model of fault rupture zone including geometry of the fault plane and asperity regions is then defined (see FIGURE 2). The geometry is essential to outline the earthquake source zone, whilst a so-called asperity zone determines the areas of concentrated slips within the fault plane. In general, modeling an earthquake rupture process in terms of earthquake source and asperity zones for the future tsunamigenic earthquakes in the Mentawai-Sunda region is complicated and has significant uncertainty (Natawidjaja., 2006; Griffin et al., 2016). In this study, the future earthquake source area in the Mentawai segment is defined using the fault rupture areas of the historical subduction earthquakes in the Sunda subduction zone (see Muhammad et al., 2016 for details).

Firstly, a generic fault model covering the entire region of the Mentawai segment with a size of 920 km in length and 250 km in width is constructed (see FIGURE 1B). Numerous megathrust earthquakes can be further generated within the generic fault model. This generic fault plane is consistent with the results of extensive geodetic, paleo-geodetic, paleo-seismic, and numerical studies (Nalbant et al., 2005; Natawidjaja et al., 2006; Chlieh et al., 2008; Sieh et al., 2008; Philibosian et al., 2014).

Nat. Hazards Earth Syst. Sci. Discuss., doi:10.5194/nhess-2017-75, 2017
Manuscript under review for journal Nat. Hazards Earth Syst. Sci.
Discussion started: 4 May 2017

The depth of fault plane ranges from 3 km to 50 km with a regular strike angle (i.e. 325°). The dip angle varies from 8° to 16° depending on the depth, e.g. the dip angle is larger as the depth increases. The properties of the fault plane are consistent with the previous investigations. For instance, the depth is comparable with the source models of the past Mentawai-Sunda subduction earthquakes and the strike/dip angles are in line with the slab models of the Sunda subduction zone developed by the USGS. (Newman et al., 2011; Satake et al., 2013; Philibosian et al., 2014; Yue et al., 2014; Hayes et al., 2009, 2012). In addition, to stochastically generate the earthquake sources, the fault plane is divided into 10 km by 10 km sub-faults (see FIGURE 1B).

Secondly, within the fault plane of the source zone, asperity zones are set up. The asperity zones reflect the regional seismological knowledge of earthquake ruptures. Understanding the rupture process of past seismicity in the Mentawai segment is essential to determine the asperity zones. Based on the past seismicity, the most likely asperity zones for the future tsunamigenic earthquake events in the Mentawai segment are located in the rupture areas of the 1797 and 1833 events since these two events were the last tsunamigenic earthquake events in the Mentawai-Sunda region (Borrerro et al., 2006; Natawidjaja et al., 2006; McCloskey et al., 2008). An area having 300 km long extended from 0.5°S to 3.2°S of the Mentawai segment (see FIGURE 1A) was determined as the asperity zone of the 1797 event based on the geodetic and paleo-geodetic measurements. On the other hand, an area having 320 km long extended from 2.1°S to 5°S (see FIGURE 1A) was inferred as the asperity zone of the 1833 event (Natawidjaja et al., 2006; Philibosian et al., 2014). Note that the 1797 event was found to produce more significant tsunami impacts in Padang than the 1833 event (Borrero et al., 2006; Natawidjaja et al., 2006; McCloskey et al., 2008). Consequently, in this study, the 1797 asperity zone is adopted to generate the future stochastic earthquake source models. In addition, in terms of selected magnitude scenarios, three scenario magnitudes are considered: M_w 8.5, M_w 8.75, and M_w 9.0.

2.1.2 Stochastic tsunami simulation

The stochastic tsunami simulation involves two main processes: (1) stochastic earthquake source model generation and (2) Monte Carlo tsunami simulation (see FIGURE 2). For generating realistic source models stochastically, regional seismological characteristics of Sumatra are analyzed. It is carried out by estimating earthquake source properties including geometry (fault length, L and fault width, W), slip statistics (mean slip, D_a, maximum slip, D_m, and Box-Cox parameter), and spatial heterogeneity parameters (correlation length along strike direction, A_x, correlation length along dip direction, A_z, and Hurst number, H). Those parameters are calculated using the effective dimension analysis method (Mai and Beroza, 2000), Box-Cox analysis (Goda et al., 2014), and spectral analysis (Mai and Beroza, 2002); see Muhammad et al. (2016) for the details.

Subsequently, the calculated regional earthquake source parameters are compared against the global scaling relationships developed by Goda et al. (2016) to examine the adequacy of the global models to the Mentawai-Sunda region. Muhammad et al. (2016) concluded that the regional earthquake source parameters calculated from the 19 past Sunda earthquakes are in good agreement with these scaling relationships; subsequently, the global models are adopted in this study.

Nat. Hazards Earth Syst. Sci. Discuss., doi:10.5194/nhess-2017-75, 2017
Manuscript under review for journal Nat. Hazards Earth Syst. Sci.
Discussion started: 4 May 2017

Natural Hazards and Earth System Sciences Discussions

A set of 100 source models is then generated for each magnitude. Therefore, the total number of the stochastic earthquake slip models used in this study is 300.

For a given stochastic source model, the initial deformation of seabed is calculated by considering both horizontal and vertical displacements of the seafloor using Okada (1985) and Tanioka and Satake (1996). Tsunami modeling is then carried out by solving non-linear shallow water equations with run up (Equations 1 to 3). A staggered leap-frog scheme is adopted to solve the governing equations (Goto et al., 1997).

$$\frac{\partial \eta}{\partial t} + \frac{\partial M}{\partial x} + \frac{\partial N}{\partial y} = 0 \,, \tag{1}$$

$$\frac{\partial M}{\partial t} + \frac{\partial}{\partial x}\left(\frac{M^2}{D}\right) + \frac{\partial}{\partial y}\left(\frac{MN}{D}\right) + gD\frac{\partial \eta}{\partial x} + \frac{gn^2}{D^{7/3}}M\sqrt{M^2+N^2} = 0 \,, \tag{2}$$

$$\frac{\partial N}{\partial t} + \frac{\partial}{\partial x}\left(\frac{MN}{D}\right) + \frac{\partial}{\partial y}\left(\frac{N^2}{D}\right) + gD\frac{\partial \eta}{\partial y} + \frac{gn^2}{D^{7/3}}N\sqrt{M^2+N^2} = 0 \,, \tag{3}$$

where $D = h + \eta$ representing the total water depth, in which h and η are the water depth and the tsunami height above the reference sea level, respectively, g is the gravitational acceleration, and n is the Manning's roughness coefficient. The discharge fluxes (i.e. M and N) are obtained from the integration of velocity in x (u) and y (v) directions over the water depth (Equations 4 and 5).

$$M = \int_{-h}^{\eta} u \, dz = u(h+\eta) = uD \,, \tag{4}$$

$$N = \int_{-h}^{\eta} v \, dz = v(h+\eta) = vD \,, \tag{5}$$

Moreover, DEM and bathymetry datasets are further developed to run the stochastic tsunami simulation. In this study, the DEM5 is adopted as land elevation data (see Section 2.13 for the details), whilst for bathymetry, the GEBCO2014 dataset (http://www.gebco.net/data_and_products/gridded_bathymetry_data/) and a 3-m Padang bathymetry dataset are combined. Four nested grids, i.e. 1350 m, 450 m, 150 m, and 50 m, being produced from linear interpolation of these datasets, are used to run the tsunami simulation. A roughness coefficient of 0.025 $m^{-1/3}s$ for water and 0.06 $m^{-1/3}s$ for land are adopted to model the surfaces roughness effects on tsunami flows (Griffin et al., 2015). By assuming instantaneous fault rupture, the duration and time step of tsunami simulation are then defined as 2 hours and 0.5 s, respectively. It satisfies the Courant-Friedrichs-Lewys (C.F.L.) criterion for the bathymetry and elevation data for the Mentawai region. The Monte Carlo tsunami simulation is finally performed using different stochastic earthquake source scenarios.

2.1.3 Effect of Digital Elevation Model on tsunami inundation modeling

An accurate DEM is essential for tsunami simulation and is particularly critical in calculating tsunami inundation depths. Recently, several international organizations and consortia have produced global DEM datasets, including GTOPO30, SRTM30, SRTM3v2, SRTM3v4, SRTM1, and GDEM2. Currently, the SRTM1 (https://lta.cr.usgs.gov/SRTM1Arc) and

Nat. Hazards Earth Syst. Sci. Discuss., doi:10.5194/nhess-2017-75, 2017
Manuscript under review for journal Nat. Hazards Earth Syst. Sci.
Discussion started: 4 May 2017

Natural Hazards and Earth System Sciences Discussions

GDEM2 (https://asterweb.jpl.nasa.gov/gdem.asp) with the resolution of 1 arc-sec (~30 m) are the best available global DEM datasets and widely used for land elevation data in tsunami simulation (Satake et al., 2013; Yue et al., 2014). In general, the range of numerical processes employed in the compilation of DEMs can have a major influence on the magnitude of errors. Both epistemic and aleatory noise can be present. For instance, the average vertical errors of the SRTM1 and GDEM2 are in the range of 10 m (Tachikawa et al., 2011; Satge et al., 2015). Because tsunami evacuation plans are mainly developed based on the inundation results, the effect of DEM on tsunami inundation modeling is assessed before presenting the main tsunami simulation results in Section 3. In our study, the baseline DEM is the local DEM5. The DEM5 dataset was developed from GPS measurements and high-resolution satellite imagery to produce the DEM profile of Padang, particularly near the coastal line (see FIGURE 4A). A vertical error of 0.2 m was found in this dataset. Hence, the DEM5 is reliable to represent the land elevation of Padang (Taubenbock et al., 2009; Schlurmann et al., 2010).

In this section, two global DEM datasets, i.e. SRTM1 and GDEM2, are adopted to study the effect of DEMs on tsunami inundation modeling in the Padang areas (see FIGURE 4B and FIGURE 4C). The elevation differences between the DEM5 and the two global datasets (i.e. SRTM1 and GDEM2) are firstly assessed and discussed. Then, the differences on tsunami inundation results from these three datasets are further presented. Note that the bathymetry dataset (GEBCO2014) is common for all three cases. The considered source model is one realization from the 100 stochastic earthquake sources in the Mentawai-Sunda zone for the M_w 9.0 scenario. This is shown in FIGURE 3B; the maximum slip of the chosen model reaches 25 m with the fault size of 450 km in length and 250 km in width.

The elevation differences of the SRTM1 and the GDEM2 datasets with respect to the reference DEM5 data are presented in FIGURE 5A and FIGURE 5B, respectively. The elevation differences are calculated by taking the elevation differences between the global DEM datasets (i.e. SRTM1 and GDEM2) and the reference data. Several statistics including minimum, maximum, mean difference, absolute mean difference, and Root Mean Square Error (RMSE) values, are calculated for each global DEM dataset and presented in Table 1. The difference with the reference data in terms of maximum elevation value for the SRTM1 is 7 m. This is smaller than 12 m for the GDEM2 dataset. The other three statistical scores, i.e. the mean difference, the absolute mean difference, and the RMSE, for the SRTM1 are also smaller than the GDEM2. For instance, the RMSE of SRTM1 is 4.27 m, which is smaller than 7.46 m for the GDEM2. In general, the SRTM1 performs better than the GDEM2. However, the RMSE scores of 4.27 m and 7.46 m may lead to inaccurate modeling of inundation in land especially in low-lying areas where the elevation is below 10 m.

Subsequently, to evaluate the effect of DEMs on inundation modeling, FIGURE 6 illustrates inundation maps in Padang based on three different DEMs, i.e. the DEM5 (FIGURE 6A), the SRTM1 (FIGURE 6B), and the GDEM2 (FIGURE 6C). Total inundation areas are also presented in FIGURE 6. The inundation maps indicate that the global DEM datasets (i.e. SRTM1 and GDEM2) underestimate the inundation areas significantly. The total inundation area of SRTM1 is less than a half of the DEM5 (i.e. 7.32 km^2 in comparison to 16.04 km^2 for the DEM5). On the other hand, the GDEM2 performs worse than the SRTM1 with only 0.74 km^2 of total inundation area. The inundation difference for the SRTM1 is mainly because of relatively high elevation differences (~5 m) between the SRTM1 and the DEM5 near the coastal region (see FIGURE 5A). Moreover, for the

GDEM2, the significant differences are mainly due to the overlapping land areas in the seaside area of the GDEM2 dataset which prevent the tsunami flow to go further in land (see black rectangle in FIGURE 4C). In addition, significant differences of inundation areas found in the GDEM2 dataset are also due to high RMSE (7.42 m) and elevation differences (~8 m) in low-lying areas near the coastal line of Padang. Consequently, it is highly recommended to use an accurate local elevation dataset merged for tsunami inundation modeling and hence, the DEM5 dataset is adopted in this study as land data.

2.2 Development of evacuation plans

In general, an evacuation plan in tsunami-prone areas consists of horizontal evacuation and vertical evacuation. Horizontal evacuation is to take refugee to the safe regions horizontally (to higher elevation areas and further away from the coast line) which are not expected to be inundated by the tsunami (Scheer et al., 2012; Wang et al., 2016). Usually, horizontal evacuation takes a long time for all evacuees to complete. On the other hand, vertical evacuation is the evacuation to either the natural high ground (e.g. hill) or a multi-story building (e.g. TES).

2.2.1 Evaluation of building height and capacity

The initial steps for developing an effective evacuation plan are to produce tsunami inundation maps and to compare them with building heights of the existing TES in Padang. In this study, the inundation maps are developed at three different percentiles, i.e. the 10^{th} percentile, the 50^{th} percentile and the 90^{th} percentile out of 100 stochastic tsunami simulation results, for a given magnitude scenario. Table 2 presents a summary of the TES in Padang. The total capacity of a TES building in Table 2 is estimated based on field surveys in 2009 and 2013 by assuming that 1 person needs an evacuation area of 1.65 m^2 (Sutikno et al., 2010; Kurniawan et al., 2014). The evaluation of the building height aims at assessing whether the existing TES buildings in Padang have sufficient heights against the tsunami inundation depth (Scheer et al., 2011, 2012; FEMA P-646, 2012). The safe height (H_{safe}) parameter is calculated as (Scheer et al., 2011, 2012; FEMA P-646, 2012):

$$H_{safe}(X,Y) = (H_{max}(X,Y) \times 1.30) + 1\,m), \quad (6)$$

where H_{max} is the maximum inundation depth at the coordinate location (X and Y) of a TES. The TES is considered to have sufficient height for tsunami evacuation shelter if its height is greater than the safe height.

It is also important to determine the TES capacity for accommodating the evacuees during the tsunamigenic event (Budiarjo, 2006; Widyaningrum, 2009; Dewi, 2012). This evaluation is conducted by calculating the TES capacity (TESC):

$$TESC = (EAF \times NF)/SpP, \quad (7)$$

where EAF is the existing evacuation area at each floor and NF is the total number of floor excluding inundated floor (Budiarjo, 2006; Widyaningrum, 2009; Dewi, 2012). Several assumptions are made to calculate the TES building capacity, which are the following:

1. Floors of the TES buildings are categorized into two floor types, i.e. unsafe floor and evacuation floor. The unsafe floor is the floor that is inundated by the tsunami, whilst the evacuation floor is the floor for evacuation areas.
2. Inundated floor is considered to be unsafe for evacuation and hence, is excluded from building capacity estimation during the tsunamigenic event.
3. Space needed per person (SpP) at the evacuation areas in each TES building is 1 m^2 determined based on 0.8 m^2 for stay and 0.2 m^2 for circulation (BAPPENAS, 2005; Budiarjo, 2006; Widyaningrum, 2009; Dewi, 2012). This value is similar to that recommended by (FEMA P-646, 2012), i.e. 0.93 m^2 per person.
4. Existing evacuation area in each floor of the TES building is assumed to be equal for all floors because only total evacuation area data for the whole building are available.

2.2.2 Evacuation time maps

Thirdly, horizontal and vertical tsunami evacuation time maps are developed based on the total evacuation time (TET), which are calculated by summing initial reaction time (IRT) and evacuation time (ET).

$$TET = IRT + ET, \quad (8)$$

$$IRT = DT + NT + RT, \quad (9)$$

The initial reaction time is the actual response time for the community to start the evacuation, whilst the evacuation time is the time needed for the community to evacuate to the safe areas. In principle, three components are considered to calculate the initial reaction time (IRT) during the tsunamigenic event including institutional decision time (DT), institutional notification time (NT), and reaction time of the community (RT), as presented in Equation (9). The institutional times (DT and NT) are determined by the related government institution which has the authority to issue hazard warning (Charnkol and Tanaboriboon, 2006; Post et al., 2009). In Indonesia, the official institution to release tsunami warning is the Indonesia Tsunami Early Warning System of Indonesian Agency for Meteorology, Climatology and Geophysics (INA-TEWS of BMKG). The INA-TEWS normally needs 5 minutes to issue tsunami warning (Widyaningrum, 2009; Dewi, 2012). In addition, the institutional notification time is assumed to be 3 minutes, whilst the reaction time of the community is 7-10 minutes (Charnkol and Tanaboriboon, 2006; Post et al., 2009). In this study, the initial reaction time used is 15 minutes by adopting the community reaction time of 7 minutes. Moreover, a suitable range of the travel speed is found to be 0.91 m/s to 3.83 m/s, depending on the traveling method (by foot or vehicle) and the evacuees' age (Wood et al., 2012; Fraser at al., 2014). In this study, the evacuation time is calculated based on the slowest travel speed (0.91 m/s) to capture the worst scenario. The evacuation time is estimated crudely by excluding roads leading to the safe places and other essential parameters (e.g. population density and age classification). Although the approximate method is not able to capture the realistic situation of evacuation accurately, it is considered to be useful for emergency managers (e.g. regional disaster management stakeholders) to develop a city-wide tsunami evacuation plan.

Finally, the integrated evacuation time maps are developed by combining horizontal and vertical evacuation time maps. The integrated evacuation time maps are calculated by taking a minimum evacuation time between evacuations horizontally and vertically. These maps are essential for the rescue teams to consider both evacuation options and subsequently may reduce the casualties during the tsunami event.

3 Results

The main results that are discussed in this section are focused on (1) tsunami hazard level in Padang produced from all earthquake scenarios (M_w 8.5, 8.75, and 9.0), (2) assessment of TES in Padang for all three scenario magnitudes, and (3) horizontal, vertical, and integrated evacuation time maps during the tsunamigenic event using the M_w 9.0 scenario.

3.1 Tsunami hazard level in Padang

The tsunami hazard level in Padang is investigated by assessing the tsunami height and depth produced from the stochastic tsunami simulations for three magnitude scenarios. The height presented in this study is the height of water flow above the mean sea level, whilst the depth refers to the water flow height above the ground. Firstly, the maximum inundation depth maps for all scenarios along with the maximum inundation depth maps for the areas above 1 m depth are presented and discussed. Secondly, the inundation heights along the coastal line and three main rivers in Padang, i.e. (1) Kuranji river, (2) Banda Bakali river, and (3) Arau river, are discussed (see FIGURE 3A). The inundation footprints along the rivers are concerned because the tsunami flow may penetrate far inland through the rivers, as observed in the 2011 Tohoku event (Mori et al., 2011; Tanaka et al., 2014).

The maximum inundation depth maps in Padang are presented in FIGURE 7, whilst the total inundation areas for the depth above 1 m are shown in FIGURE 8. Three maps in each magnitude scenario are for the 10th percentile (left panel), the 50th percentile (central panel), and the 90th percentile (right panel). FIGURE 7A shows that the tsunami impacts for the case of M_w 8.5 are insignificant in Padang. The total inundated areas exhibited in the 90th percentile map of the M_w 8.5 scenario are relatively minor (only 3.12 km^2). Those inundated areas are concentrated near the coastal line of Padang with the total inundation areas above 1 m depth is only 0.94 km^2 (see the right panel of FIGURE 8A). These results are much smaller than the maximum tsunami inundation areas for the same magnitude scenario (M_w 8.5) produced by the GITEWS (Goseberg and Schulrmann, 2009; Taubenbock et al., 2009; Schlurmann et al., 2010). This is due to the use of deterministic source scenarios in which large earthquake slips are placed very close to Padang (less than 20 km). Consequently, the considered earthquake scenarios used in the GITEWS project may over-predict the tsunami inundation areas. In addition, the inundation areas increase significantly from the M_w 8.5 scenario to the M_w 8.75 scenario as shown in the 90th percentile maps. The maximum total inundation areas for the M_w 8.75 case are about four times larger than the M_w 8.5 scenario (increasing from 3.12 km^2 to 11.59 km^2). The inundation areas above 1 m depth for the 90th percentile of the M_w 8.75 case also increase drastically to 8.52 km^2 as presented in the right panel of FIGURE 8B.

Nat. Hazards Earth Syst. Sci. Discuss., doi:10.5194/nhess-2017-75, 2017
Manuscript under review for journal Nat. Hazards Earth Syst. Sci.
Discussion started: 4 May 2017

Moreover, the tsunami effects are found to be much more significant for the M_w 9.0 scenario. The total inundation areas above 1 m depth reach 16.55 km^2 at the 90th percentile. The evacuation from the inundated areas might be very difficult in such a situation. On the other hand, in general, the maximum tsunami-affected areas produced from the stochastic tsunami simulations are larger than the results from the GITEWS project which are used to build the current evacuation plan in Padang (Taubenbock et al. 2009; Schlurmann et al., 2010). The existing tsunami evacuation plan may oversimplify the future tsunamigenic event and therefore, the improvements of these maps are highly desirable to capture the worst scenarios that may occur in the future.

To capture the variability of inundation extent in Padang, FIGURE 9 to FIGURE 12 show the inundation height profiles along the coastal line and three rivers in Padang. The length of the Kuranji, Banda Bakali, and Arau rivers from their river-mouths are 1.4 km, 1.7 km, and 2.45 km, respectively. In general, high variability of inundation heights is found along the coastal line of Padang (FIGURE 9). The 10th rank from the three magnitude scenarios show that the tsunami wave heights along the coastal line range from 0 m (for the M_w 8.5 scenario) to 3 m (for the M_w 9.0 scenario). By contrast, for the 90th rank of the M_w 9.0 scenario, the maximum tsunami height reaches 10 m. Moreover, the inundation heights along the rivers (see FIGURE 10, FIGURE 11, and FIGURE 12) also show high variability of the wave height, ranging between 0 m and 10 m. The 10th and 50th percentiles of inundation heights for the M_w 8.5 and M_w 8.75 scenarios tend to decrease to zero as the locations go further inland. However, the tsunami inundation heights remain almost constant along the rivers for the M_w 9.0 case, as presented for the 50th and 90th ranks. This highlights that the tsunami waves can run up the rivers by more than 2 km from the coastal line and hence, people who live along the rivers may be more affected. In addition, the inundation height profiles along the coastal line and the rivers in Padang show that the stochastic tsunami simulation method can capture the uncertainty of the inundation extent. Therefore, the implementation of the stochastic tsunami simulation method for predicting the future events is highly desirable for preparing more effective and robust mitigation plans.

3.2 Assessment of tsunami evacuation shelters

Currently, in east and north of Padang, 23 TES have been set up/designated by the National Agency for Disaster Management (BNPB) of Padang (see Table 2). However, their adequacy was evaluated under the design scenarios only. Consequently, re-assessment of TES in Padang is highly desirable by taking into account uncertainties associated with the tsunami hazards. This will provide residents and emergency/rescue teams with valuable information regarding the current tsunami risk exposure in Padang. In this section, the existing TES is assessed by comparing the building height of a TES building against the inundation depth and the TES building capacity during three scenarios of the worst magnitude event (M_w 9.0). In addition, the tsunami inundation depth variability at each TES building is also discussed.

The variability of tsunami inundation depth at each TES is shown in FIGURE 13. The tsunami impacts to all TES are insignificant in the case of M_w 8.5 for all percentiles. The tsunami depths at the TES locations from 100 tsunami simulations are zero for the majority of the cases. The tsunami impacts start to increase for the M_w 8.75 scenario. In this scenario, the variability of inundation depth at several TES (e.g. shelter numbers 16, 17, 20, and 23) ranges from 0 m to more than 5 m.

Nat. Hazards Earth Syst. Sci. Discuss., doi:10.5194/nhess-2017-75, 2017
Manuscript under review for journal Nat. Hazards Earth Syst. Sci.
Discussion started: 4 May 2017

Natural Hazards and Earth System Sciences Discussions

However, the 90th percentile values of tsunami depth for all TES are still below 5 m. On the other hand, the significant impacts are shown from the variability of tsunami inundation depth for the M_w 9.0 scenario. Three out of the 23 TES, i.e. shelter numbers 1, 15, and 22, with the building height of 10 m may be significantly affected by the tsunami. The depth variability in those three buildings ranges from 0 m to nearly 10 m (see FIGURE 13C). Additional information regarding the depth variability at the TES locations also presented in FIGURE 14 developed from the M_w 9.0 scenario. Eleven from the 23 TES locations (i.e. shelter numbers 1, 2, 3, 4, 10, 13, 15, 16, 17, 20, and 23) are chosen to illustrate the depth variability and tsunami arrival time at the TES sites. These stations are located close to the coastal line and the rivers (see FIGURE 3) and hence, are majorly affected by the tsunami. FIGURE 14 shows that several stations (e.g. shelter numbers 16, 17, and 20) are inundated by a maximum depth of nearly 10 m with the arrival times of about 15 minutes based on the 90th rank of the M_w 9.0 scenario.

Subsequently, the TES is further assessed using the obtained tsunami depths from three percentiles of the M_w 9.0 scenario, i.e. the 10th, 50th, and 90th percentile cases. Table 3 presents the comparison of TES building heights with the estimated inundation depths for three percentiles of the M_w 9.0 scenario. In addition, to capture the shortest tsunami arrival time at each TES stations, the tsunami arrival times calculated based on the 90th rank of the M_w 9.0 case are also presented in Table 3. In short, all TES has sufficient heights as tsunami evacuation shelters because all the TES building heights are above the safe height. However, the tsunami arrival times at several shelters (shelter numbers 4, 16, 17, and 20) are relatively short (about 15-18 minutes) and hence, quick evacuation responses are needed in these shelter areas. On the other hand, the estimation of TES building capacity may capture another point of view regarding the adequacy of existing TES for evacuation. Table 4, presents the estimation of TES building capacity during the tsunami event considering the 10th percentile, the 50th percentile, and the 90th percentile, respectively. In terms of capacity, all the TES buildings can be used for vertical evacuation during the 10th rank event. However, for the 50th percentile case, the shelter number 1 (sport center of UNP) may not be operational, whilst for the 90th percentile case, shelter numbers 1 and 15 (Elementary school of 24 Padang) are unable to accommodate evacuees since all floors will be inundated. Note that, for the shelter number 1, there is only one floor since most of the building areas are used for the sport arena. In terms of capacity, during the 50th and 90th rank cases, the possible maximum capacity to be accommodated at all TES buildings are only about 72,000 and 48,000 people, respectively. These numbers are still insufficient in comparison to the total population in the coastal region of Padang (i.e. ~200,000 people). Therefore, it is highly recommended to increase the number of TES near the coastal areas in Padang. Importantly, the TES assessment results highlight that the stochastic tsunami simulation method is able to capture the uncertainty of the future tsunamigenic impacts and hence, is essential to use this method for building an effective tsunami mitigation plan.

3.3 Tsunami evacuation maps

This section presents the tsunami evacuation maps based on the stochastic tsunami inundation depths in Padang. The developed tsunami evacuation maps consist of tsunami inundation maps and horizontal, vertical, and integrated evacuation time maps to the safe zones. Three scenarios are considered to develop tsunami evacuation time maps for the M_w 9.0 scenario, i.e. the 10th percentile, the 50th percentile, and the 90th percentile. Note that the tsunami evacuation time maps developed in this section are

based on the total evacuation time as presented in **S**ection 2.2.2. The M_w 9.0 scenario is chosen because it causes the most significant tsunami impacts in Padang (see inundation maps in FIGURE 7).

FIGURE 7C shows tsunami inundation maps in Padang, whilst FIGURE 15 illustrates tsunami evacuation time maps to the safe zones in Padang for the 10th percentile (FIGURE 15A), the 50th percentile (FIGURE 15B), and the 90th percentile (FIGURE 15C). The horizontal tsunami evacuation time to the safe areas is calculated and is used to produce the tsunami evacuation time maps. The evacuation speed during the disaster event is chosen as 0.91 m/s. The total evacuation time in the 10th percentile case is sufficient to evacuate people from the coastal areas to the safe zone since the maximum evacuation time during this scenario event is about 25 minutes (see FIGURE 15A). For the 50th percentile case, some people located closer to the coastal line may need more than 30 minutes for evacuation (see FIGURE 15B). The most critical condition occurs in the case of the 90th percentile. A large population will need more than 50 minutes to evacuate to the safe zone and hence, the vertical evacuation shelters are necessary to save the people residing in those areas.

Based on the TES assessment results, the vertical and integration evacuation time maps are further developed to investigate the possibility of reducing evacuation time to the safe areas. FIGURE 15D and FIGURE 15E show the vertical and integrated tsunami evacuation time maps to the TES locations. The shelter numbers 1 and 15 are excluded while vertical and integration tsunami evacuation time maps are developed because those shelters may be inundated during the worst tsunamigenic event (the 90th percentile of the M_w 9.0 scenario). In general, the vertical evacuation time map highlights that those shelters can only be accessed by the community located near the shelters (FIGURE 15D). In addition, the integrated map shows that the availability of shelters is essential to save those residents in the critical regions (see FIGURE 15E). Generally, by incorporating the vertical evacuation shelters and reducing the initial reaction time, the total evacuation time can be shorter. Therefore, besides increasing the number of TES buildings in Padang, large-scale tsunami evacuation drills in coastal community must be conducted to improve awareness of the tsunami hazard in Padang. Consequently, the casualties due to significant tsunamigenic events can be reduced.

4 Conclusions and outlook

The main purpose of this study was to develop effective tsunami evacuation plans in Padang based on the stochastic earthquake scenarios. Rigorous tsunami hazard assessments in Padang have been carried out using a novel stochastic tsunami simulation method to estimate the tsunami hazard level in Padang using three magnitude scenarios including M_w 8.5, M_w 8.75, and M_w 9.0. The stochastic earthquake scenarios were generated by adopting an asperity zone from the 1797 historical event and by considering the uncertainty and dependency of earthquake source parameters. For each magnitude, 100 stochastic earthquake source scenarios (300 models in total) were generated and implemented to run the Monte Carlo tsunami simulation. The assessment of tsunami hazard in Padang was then conducted based on the stochastic tsunami inundation depth (vertical relative distance from water free-surface to ground). Subsequently, the assessment of TES in Padang was carried out to evaluate the adequacy during the critical tsunami events by comparing the height of the existing TES buildings with the safe height and by

estimating the TES building capacity. Finally, the hazard level assessment results were used to construct the tsunami inundation depth maps and tsunami evacuation time maps (i.e. horizontal, vertical, and integrated evacuation time maps) to better inform emergency response and rescue teams of current tsunami risks to residents in Padang. The evacuation time maps were developed for the three percentile levels (i.e. 10^{th}, 50^{th}, and 90^{th}) of the M_w 9.0 scenario.

For the M_w 9.0 scenario, the tsunami inundation areas in Padang ranged from 4.27 km^2 for the 10^{th} percentile to 19.43 km^2 for the 90^{th} percentile with a maximum inundation depth reaching 10 m. The results clearly demonstrated that Padang may face a significant impact of the tsunami in the case of the low-probability high-consequence events. People who live near the coast will require about 60 minutes evacuating to the safe zone (i.e. to inland high ground). In such situations, resistant vertical evacuation structures should be designed and constructed in the populated areas of Padang along the coast. The results from the assessment of the existing 23 TES in Padang indicated that all TES buildings have sufficient design heights against anticipated tsunamis. However, the capacity may be insufficient to accommodate a large number of population in the coastal region and hence, the number of TES must be increased.

Lastly, although assessments for developing evacuation plans in Padang have been conducted in this study using the results of rigorous stochastic tsunami simulations, some limitations need to be addressed in future studies. These include: (1) tsunami hazard simulations should be conducted using high-resolution DEM (e.g. 10 m), and (2) other tsunami hazard parameters, e.g. flow velocity and momentum flux, as well as other tsunami evacuation parameters, e.g. population distribution and road access, should be taken into account when assessing the adequacy of TES in Padang.

Acknowledgments

The first author is grateful to the Directorate General of Resources for Science, Technology and Higher Education, Ministry of Research, Technology and Higher Education of Indonesia which sponsor his PhD study. This work is also funded by the Engineering and Physical Sciences Research Council (EP/M001067/1). The authors are grateful to Sigit Sutikno who provided the TES survey data in Padang. The bathymetry and elevation data for the Sumatra region were obtained from the GEBCO2014 database (http://www.gebco.net/data_and_products/gridded_bathymetry_data/), the SRTM1 (https://lta.cr.usgs.gov/SRTM1Arc) database and the GDEM2 database (https://asterweb.jpl.nasa.gov/gdem.asp), respectively.

References

BAPPENAS: Master Plan for the rehabilitation and reconstruction of the regions and communities of the province of Nanggroe Aceh Darussalam and the Islands of Nias, Province of North Sumatera. Jakarta, BAPPENAS: 126 pages, 2005.

Borrero, J. C., Sieh, K., Chlieh, M., and Synolakis, C. E.: Tsunami inundation modeling for western Sumatra, Proc. Nat. Acad. Sci. U.S.A., 103, 19673–19677, doi:10.1073/pnas.0604069103, 2006.

Budiarjo, A.: Evacuation shelter building planning for tsunami prone area: a case study of Meulaboh city, Indonesia. Enschede, ITC: 112 pages, 2006.

Charnkol, T. and Tanaboriboon, Y.: Tsunami evacuation behavior analysis: one step of transportation disaster Response, IATSS Res., 30, 83-96, 2006.

Chlieh, M., Avouac, J. P., Sieh, K., Natawidjaja, D. H., and Galetzka, J.: Heterogeneous coupling of the Sumatran megathrust constrained by geodetic and paleogeodetic measurements, J. Geophys. Res., 113, B05305: 1–31, doi:10.1029/2007JB004981, 2008.

Dewi, R. S.: A-Gis Based approach of an evacuation model for tsunami risk reduction, IDRiM J., 2, 108-139, doi:10.5595/idrim.2012.0023, 2012.

FEMA (Federal Emergency Management Agency) P-646: Guidelines for Design of Structures for Vertical Evacuation From Tsunamis (second ed.) Federal Emergency Management Agency, Washington, D.C., 2012.

Gallegos, H. A., Schubert, J. E., and Sanders, B. F.: Two-dimensional, high-resolution modeling of urban dam-break flooding: a case study of Baldwin Hills, California. Adv. Water Resour. 32, 1323–1335. doi: 10.1016/j.advwatres.2009.05.008, 2009.

Goda, K., Mai, P. M., Yasuda, T., and Mori, N.: Sensitivity of tsunami wave profiles and inundation simulations to earthquake slip and fault geometry for the 2011 Tohoku earthquake, Earth Planet Space, 66, 105. doi:10.1186/1880-5981-66-105, 2014.

Goda, K., Yasuda, T., Mori, N., and Maruyama, T.: New Scaling Relationships of Earthquake Source Parameters for Stochastic Tsunami Simulation, Coast. Eng. J., 58, 1-40, doi:10.1142/S0578563416500108, 2016.

Goseberg, N. and Schulrmann, T.: Tsunami hazard mapping and risk assessment for the city of Padang/West Sumatra, Meeting of Disaster Risk Reduction for Natural Hazard, London, November 2009. Availaible from: http://www.ucl.ac.uk/drrconference/presentations/TSchlurmann.pdf

Goto, C., Ogawa, Y., Shuto, N., and Imamura, F.: Numerical method of tsunami simulation with the leap-frog scheme. IOC Manual, UNESCO, 35, Paris, France, 1997.

Griffin, J., Latief, H., Kongko, W., Harig, S., Horspool, N., Hanung, R., Rojali, A., Maher, N., Fuchs, A., Hossen, J., Upi, S., Edi, Dewanto, S., Rakowsky, N., and Cummins, P.: An evaluation of onshore digital elevation models for modeling tsunami inundation zones, Front. Earth Sci. 3:32. doi:10.3389/feart.2015.00032, 2015.

Griffin, J. D., Pranantyo, I. R., Kongko, W., Haunan, A., Robiana, R., Miller, Davies, G., Horspool, N., Maemunah, I., Widjaja, W.B., Natawidjaja, D.H., and Latief, H.: Assessing tsunami hazard using heterogeneous slip models in the Mentawai Islands, Indonesia. In P. R. & Meilano, I. (eds) Geohazards in Indonesia: Earth Science for Disaster Risk Reduction. Geological Society, London, Special Publications, 441. doi:10.1144/SP441.3, 2016.

Hayes, G. P., Wald, D. J., and Keranen, K.: Advancing techniques to constrain the geometry of the seismic rupture plane on subduction interfaces a priori - higher order functional fits, Geochem. Geophys. Geosyst., 10, Q09006, doi:10.1029/2009GC002633, 2009.

Hayes, G. P., Wald, D. J., and Johnson, R. L.: Slab1.0: A three-dimensional model of global subduction zone geometries, J. Geophys. Res., 117, B01302, doi:10.1029/2011JB008524, 2012.

Imamura, F., Muhari, A., Mas, E., Pradono, M. H., Post, J., and Sugimoto, M.: Tsunami Disaster Mitigation by Integrating Comprehensive Countermeasures in Padang City, Indonesia, J. Disaster Res., 7, 48-64, 2011.

Kazama, M. and Noda, T.: Damage statistics (Summary of the 2011 off the Pacific Coast of Tohoku Earthquake damage), Soils Found., 52, 780–792, http://dx.doi.org/10.1016/j.sandf.2012.11.003, 2012.

Konca, A. O., Hjorleifsdottir, V., Song, T. A., Avouac, J. P., Helmberger, D. V., Ji, C., Sieh, K., Briggs, R., and Meltzner, A.: Rupture kinematics of the 2005, Mw 8.6, Nias-Simeulue earthquake from the joint inversion of seismic and geodetic data, Bull. Seismol. Soc. Am., 97, S307–S322, doi:10.1785/0120050632, 2007.

Kurniawan, A. A., Sutikno, S., and Rinaldi: Evaluasi Kapasitas Shelter Evakuasi Untuk Bencana Tsunami Di Kota Padang Berbasis Sistem Imformasi Geografis (SIG), Journal Online Mahasiswa, 1, 1-9, 2014.

Lewis, M., Bates, P., Horsburgh, K., Neal, J., and Schumann, G.: A storm surge inundation model of the northern Bay of Bengal using publicly available data. Q. J. R. Meteorol. Soc. 139, 358–369. doi: 10.1002/qj.2040, 2013.

Mai, P. M. and Beroza, G. C.: Source scaling properties from finite-fault-rupture models, Bull. Seismol. Res. Lett., 85, 1348–1357, doi:10.1785/0220140077, 2000.

Mai, P. M. and Beroza, G. C.: A spatial random field model to characterize complexity in earthquake slip, J. Geophys. Res. Solid. Earth, 107, ESE 10-1–ESE 10-21, doi:10.1029/2001JB000588, 2002.

McCloskey, J., Antonioli, A., Piatanesi, A., Sieh, K., Steacy, S., Nalbant, S., Coccob, M., Giunchib, C., Huanga, J. D., and Dunlop, P.: Tsunami threat in the Indian Ocean from a future megathrust earthquake west of Sumatra, Earth Planetary Sci. Lett., 265, 61–81. doi:10.1016/j.epsl.2007.09.034, 2008.

Muhammad, A., Goda, K., and Alexander, N.: Tsunami Hazard Analysis of Future Megathrust Sumatra Earthquakes in Padang, Indonesia Using Stochastic Tsunami Simulation, Front. Built Environ., 2:33. doi: 10.3389/fbuil.2016.00033, 2016.

Muhari, A., Imamura, F., Koshimura, S., and Post, J.: Examination of three practical run-up models for assessing tsunami impact on highly populated areas, Nat. Hazards Earth Syst. Sci., 11, 3107-3123, doi:10.5194/nhess-11-3107-2011, 2011.

Muhari, A., Imamura, F., Natawidjaja, D. H., Diposaptono, S., Latief, H., Post, J., and Ismail, F.A.: Tsunami mitigation efforts with pTA in West Sumatra Province, Indonesia. J. Earthq. Tsunami, 4, 341–368, doi:10.1142/S1793431110000790, 2010.

Mueller, C., Power, W., raser, S., and Wang, X.: Effects of rupture complexity on local tsunami inundation: Implications for probabilistic tsunami hazard assessment by example, J. Geophys. Res. Solid Earth, 120, 488–502, doi:10.1002/2014JB011301, 2015.

Nalbant, S. S., Steacy, S., Sieh, K., Natawidjaja, D., and McCloskey, J.: Seismology: earthquake risk on the Sunda trench, Nature, 435, 756–757, doi: 10.1038/nature435756a, 2005.

Natawidjaja, D. H., Sieh, K., Chlieh, M., Galetzka, J., Suwargadi, B. W., Cheng, H., Edwards, R. L., Avouac, J. P., and Ward, S. N.: Source parameters of the great Sumatran megathrust earthquakes of 1797 and 1833 inferred from coral microatolls, J. Geophys. Res., 111, B06403, doi:10.1029/2005JB004025, 2006.

Newman, A. V., Hayes, G., Wei, Y., and Convers, J.: The 25 October 2010 Mentawai tsunami earthquake, from real-time discriminants, finite-fault rupture, and tsunami excitation. Geophys. Res. Lett., 38, 1–7, doi:10.1029/2010GL046498, 2011.

Okada, Y.: Surface deformation due to shear and tensile faults in a half-space. Bull. Seismol. Soc. Am. 75, 1135–1154, 1985.

Philibosian, B., Sieh, K., Avouac, J. P, Natawidjaja, D. H., Chiang, H., Wu, C., Perfettini, H., Shen, C. C., Daryono, M. R., and Suwargadi, B. W.: Rupture and variable coupling behavior of the Mentawai segment of the Sunda megathrust during the super cycle culmination of 1797 to 1833. J. Geophys. Res. Solid Earth, 119, 7258–7287, doi:10.1002/2014JB011200, 2014.

Post, J., Wegscheider, S., Mück, M., Zosseder, K., Kiefl, R., Steinmetz, T., and Strunz, G.: Assessment of human immediate response capability related to tsunami threats in Indonesia at a sub-national scale, Nat. Hazards Earth Syst. Sci., 9, 1075-1086, doi:10.5194/nhess-9-1075-2009, 2009.

Raby, A., Macabuag, J., Pomonis, A., Wilkinson, S., and Rossetto, T.: Implications of the 2011 Great East Japan Tsunami on sea defence design, Int. J. Disaster Risk Reduct., 14, 332-336. doi:10.1016/j.ijdrr.2015.08.009, 2015.

Sanders, B. F.: Evaluation of on-line DEMs for flood inundation modeling. Adv. Water Resour. 30, 1831–1843. doi: 10.1016/j.advwatres.2007.02.005, 2007.

Satake, K., Nishimura, Y., Putra, P. S., Gusman, A. R., Sunendar, H., Fujii, Y., Sunendar, H., Latief, H., and Yulianto, E.: Tsunami source of the 2010 Mentawai, Indonesia earthquake inferred from tsunami field survey and waveform modeling, Pure Appl. Geophys., 170, 1567–1582, doi:10.1007/s00024-012-0536-y, 2013.

Satge, F., Bonnet, M. P., Timouk, F., Calmant, S., Pillco, R., Molina, W., Lavado-Casimiro, Arsen, A., Crétaux, J. F., and Garnier, J.: Accuracy assessment of SRTM v4 and ASTER GDEM v2 over the Altiplano watershed using ICESat/GLAS data. Int. J. Remote Sens., 36:2, 465–88, 2015.

Sutikno, S., Murakami, K., and Rinaldi: Evaluation of Tsunami Evacuation Risks in Padang City -Case Study on 2009 West Sumatera Earthquake. J. Japan Soc. Civ. Eng., 36, 267-272, doi: 10.13140/RG.2.1.3078.0964, 2010.

Scheer S. J., Gardi, A., Guillande, R., Eftichidis, G., Varela, V., de Vanssay., B., and Colbeau-Justin., L.: Handbook of tsunami evacuation planning, JCR Scientific and Technical Reports, European Union, 2011.

Scheer, S. J., Varela, V., and Eftychidis, G.: A generic framework for tsunami evacuation planning, Phys. Chem. Earth Parts A/B/C, 49, 79–91, doi:10.1016/j.pce.2011.12.001, 2012.

Schlurmann, T., Kongko, W., Goseberg, N., Natawidjaja, D. H., and Sieh, K.: Near-field tsunami hazard map padang, west sumatra: utilizing high resolution geospatial data and reasonable source scenarios. Coastal Engineering Proc., 32, 1-17. doi: doi:10.9753/icce.v32.management.26, 2010.

Sieh, K., Natawidjaja, D. H., Meltzner, A. J., Shen, C. C., Cheng, H., Li, K. S., Suwargadi, B. W., Galetzka, J., Philibosian, B., and Edwards, R. L.: Earthquake super cycles inferred from sea-level changes recorded in the corals of West Sumatra, Science, 322, 1674–1678, doi:10.1126/science.1163589, 2008.

Tachikawa, T., Kaku, M., Iwasaki, A. and Hato, M.: Characteristics of ASTER GDEM Version 2. IEEE Int. Geosci. Remote Sens. Symp. (IGARRS 2011). Vancouver, Canada, 1–4, 2011.

Tanioka, Y. and Satake, K.: Tsunami generation by horizontal displacement of ocean bottom, Geophys. Res. Lett., 23, 861–864, 1996.

Taubenbock, H., Goseberg, N., Setiadi, N., Lammel, G., Moder, F., Oczipka, M., Klupfel, H., Wahl, R., Schlurmann, T., Strunz1, G., Birkmann, J., Nagel, K., Siegert, K., Lehmann, F., Dech, S., Gress, A., and Klein, R.: "Last-Mile" preparation for a potential disaster – Interdisciplinary approach towards tsunami early warning and an evacuation information system for the coastal city of Padang, Indonesia. Nat. Hazards Earth Syst. Sci., 9, 1509–1528. doi:10.5194/nhess-9-1509-2009, 2009.

Wang, H., Mostafizi, A., Lori, Cramer, A., Cox, D., and Park, H.: An agent-based model of a multimodal near-field tsunami evacuation: Decision-making and life safety, Transportation Research Part C: Emerging Technologies, 64, 86-100, doi:10.1016/j.trc.2015.11.010, 2016.

Widyaningrum, E.: Tsunami Evacuation Planning Using Geoinformation Technology Considering Land Management Aspects, Case Study: Cilacap, Central of Java. Centre of Land and Environmental Risk Management. Munich, Technische Universität München: 87 pages, 2009.

Wood, N. J. and Schmidtlein, M. C.: Anisotropic path modeling to assess pedestrian-evacuation potential from Cascadia-related tsunamis in the US Pacific Northwest, Nat. Hazards, 62, 275-300, doi:10.1007/s11069-011-9994-2, 2012.

Wood, N. J., Jones, J., Schelling, J., and Schmidtlein, M.C.: Tsunami vertical-evacuation planning in the U.S. Pacific Northwest as a geospatial, multi-criteria decision problem, Int. J. Disaster Risk Reduct., 9, 68-83. doi:10.1016/j.ijdrr.2014.04.009, 2014.

United States Geological Survey (USGS). (2015). Latest earthquakes. http://earthquake.usgs.gov/earthquakes/map/.

Yue, H., Lay, T., Rivera, L., Bai, Y., Yamazaki, Y., Cheung, K. F., Hill, E. M., Sieh, K., Kongko, W., and Muhari, A.: Rupture process of the 2010 Mw7.8 Mentawai tsunami earthquake from joint inversion of near-field hr-GPS and teleseismic body wave recordings constrained by tsunami observations, J. Geophys. Res. Solid Earth., 119, 5574–5593, doi:10.1002/2014JB011082, 2014.

Nat. Hazards Earth Syst. Sci. Discuss., doi:10.5194/nhess-2017-75, 2017
Manuscript under review for journal Nat. Hazards Earth Syst. Sci.
Discussion started: 4 May 2017

Natural Hazards and Earth System Sciences
Discussions

Figure captions

FIGURE 1. (A) Significant seismic events in the Mentawai segment of the Sunda subduction zone (Sim: Simeulue, Ni: Nias, Ba: Batu, Sib: Sibereut, Sip: Sipora, Pag: Pagai Islands, Eng: Enggano). (B) Fault plane of the Mentawai segment source along with the asperity.
FIGURE 2. Procedures of stochastic tsunami simulation.
FIGURE 3. (A) Tsunami evacuation shelters in Padang. (B) Earthquake source models to study the effect of DEM on tsunami simulation.
FIGURE 4. Digital Elevation Model for Padang: (A) DEM5. (B) SRTM1. (C) GDEM2.
FIGURE 5. Elevation differences of global DEM datasets with respect to DEM5: (A) SRTM1. (B) GDEM2.
FIGURE 6. Inundation areas in Padang for: (A) DEM5. (B) SRTM1. (C) GDEM2 (IA = total inundation areas).
FIGURE 7. Inundation depth maps in Padang: (A) M_w 8.5 scenario. (B) M_w 8.75 scenario. (C) M_w 9.0 scenario (IA = inundation area).
FIGURE 8. Inundation areas above 1 m depth in Padang: (A) M_w 8.5 scenario. (B) M_w 8.75 scenario. (C) M_w 9.0 scenario (IA = inundation area).
FIGURE 9. (A) Site location. (B) Maximum tsunami inundation height in the coastal line of Padang for the M_w 8.5 scenario. (C) Maximum tsunami inundation height in the coastal line of Padang for the M_w 8.75 scenario. (D) Maximum tsunami inundation height in the coastal line of Padang for the M_w 9.0 scenario.
FIGURE 10. (A) Site location. (B) Maximum tsunami inundation height in the first river of Padang for the M_w 8.5 scenario. (C) Maximum tsunami inundation height in the first river of Padang for the M_w 8.75 scenario. (D) Maximum tsunami inundation height in the first river of Padang for the M_w 9.0 scenario.
FIGURE 11. (A) Site location. (B) Maximum tsunami inundation height in the second river of Padang for the M_w 8.5 scenario. (C) Maximum tsunami inundation height in the second river of Padang for the M_w 8.75 scenario. (D) Maximum tsunami inundation height in the second river of Padang for the M_w 9.0 scenario.
FIGURE 12. (A) Site location. (B) Maximum tsunami inundation height in the third river of Padang for the M_w 8.5 scenario. (C) Maximum tsunami inundation height in the second river of Padang for the M_w 8.75 scenario. (D) Maximum tsunami inundation height in the third river of Padang for the M_w 9.0 scenario.
FIGURE 13. Inundation depth variability at TES stations for (A) M_w 8.5 scenario. (B) M_w 8.75 scenario. (C) M_w 9.0 scenario.
FIGURE 14. (A-K) Inundation depth variability at TES stations located near the coastal line and the rivers.
FIGURE 15. (A) Horizontal tsunami evacuation time maps in Padang for the 10^{th} percentile. (B) Horizontal tsunami evacuation time maps in Padang for the 50^{th} percentile. (C) Horizontal tsunami evacuation time maps in Padang for the 90^{th} percentile. (D) Vertical tsunami evacuation time maps in Padang for the 90^{th} percentile. (E) Integrated tsunami evacuation time maps in Padang for the 90^{th} percentile.

Nat. Hazards Earth Syst. Sci. Discuss., doi:10.5194/nhess-2017-75, 2017
Manuscript under review for journal Nat. Hazards Earth Syst. Sci.
Discussion started: 4 May 2017

Natural Hazards and Earth System Sciences Discussions

Table 1. Statistics of elevation differences between global DEM datasets (i.e. SRTM1 and GDEM2) and the reference data (DEM5).

DEM	Min (m)	Max (m)	Mean difference (m)	Absolute mean difference (m)	RMSE (m)
DEM5	0	280	-	-	-
SRTM1	0	273	1.48	3.13	4.27
GDEM2	0	268	3.96	5.69	7.46

Table 2. Tsunami evacuation shelters in Padang.

No.	Name of the shelter	Capacity (persons)	Location		Maximum height (m)	Number of floors	Evacuation area (m^2)
			Longitude	Latitude			
1	Sport centre of Universitas Negeri Padang (UNP)	1,500	100.3474	-0.89979	10	1	2475
2	Art building of UNP	2,000	100.3488	-0.89998	20	5	3300
3	DPRD province building	2,000	100.3515	-0.90628	15	3	3300
4	Post-graduate building of Universitas Bung Hatta (UBH)	2,000	100.3434	-0.90677	15	4	3300
5	Al-Azhar primary school	1,100	100.3544	-0.90924	10	3	1815
6	BPK office of West Sumatra	2,000	100.3566	-0.91127	20	4	3300
7	Office of KANWIL DITJEN perbendaharaan	2,000	100.3587	-0.9161	15	3	3300
8	Senior High School 1 of Padang	1,400	100.3539	-0.91923	10	3	2310
9	Junior High School 25 of Padang	1,000	100.3568	-0.92025	10	3	1650
10	Senior Vocational High School 5 of Padang	3,000	100.3519	-0.92178	10	3	4950
11	Grand Mosque of West Sumatra	4,000	100.3625	-0.92423	47	2	6600
12	BAPPEDA province office	1,500	100.3609	-0.92589	15	3	2475
13	Ibis hotel of Padang	3,000	100.3629	-0.9294	52	13	4950
14	PrasJal office of West Sumatra Province	5,000	100.3637	-0.92953	15	4	8250
15	Elementary School 24 of Purus	3,000	100.3546	-0.93371	10	3	4950
16	Mercure Hotel of Padang	4,000	100.3527	-0.9359	30	8	6600
17	RUSUNAWA	3,200	100.3516	-0.93681	15	5	5280
18	Governor office of West Sumatra	3,500	100.3606	-0.94116	20	4	5775
19	Office of Bank Indonesia	1,000	100.3623	-0.94336	10	2	1650
20	Nurul Haq mosque	4,000	100.3536	-0.95091	22	5	6600
21	Grand Zuri Padang Hotel	3,000	100.3641	-0.95467	25	6	4950
22	Nurul Iman mosque	1,000	100.3623	-0.95473	10	2	1650
23	Grand Inna Muara Hotel	4,000	100.357	-0.95734	25	6	6600

Nat. Hazards Earth Syst. Sci. Discuss., doi:10.5194/nhess-2017-75, 2017
Manuscript under review for journal Nat. Hazards Earth Syst. Sci.
Discussion started: 4 May 2017

Natural Hazards and Earth System Sciences
Discussions

565 Table 3. Assessment of tsunami evacuation shelters (TES) during the tsunami event in Padang.

No.	TES height (m)	10th percentile		50th percentile		90th percentile		
		Depth (m)	*H*safe (m)	Depth (m)	*H*safe (m)	Depth (m)	*H*safe (m)	Tsunami arrival time (minutes)
1	10	0	1	2.9	4.8	6	8.8	23
2	20	0.5	1.6	3.9	6	7	10.1	24
3	15	0	1	1.4	2.8	4.6	7	25
4	15	0	1	2.6	4.4	5.7	8.4	19
5	10	0	1	0.1	1.1	3.1	5	27
6	20	0	1	0	1	2.5	4.2	30
7	15	0	1	0	1	1.9	3.4	30
8	10	0	1	0.8	2.1	3.6	5.7	24
9	10	0	1	0.2	1.3	3	5	25
10	10	0	1	2.1	3.7	5.1	7.6	21
11	47	0	1	0	1	2.2	3.9	30
12	15	0	1	0	1.1	2.8	4.7	28
13	52	0	1	0.8	2.1	4	6.2	28
14	15	0	1	0	1	3.1	5.1	30
15	10	0.3	1.3	3.6	5.6	6.7	9.7	20
16	30	1.2	2.6	4.3	6.6	7.5	10.7	17
17	15	1.6	3.1	4.8	7.2	7.8	11.2	15
18	20	0	1	0.5	1.6	3.8	6	27
19	10	0	1	0	1	3	4.9	29
20	22	1.3	2.6	4	6.2	6.8	9.8	17
21	25	0	1	0.3	1.4	2.9	4.8	28
22	10	0	1	0.5	1.7	3.1	5	27
23	25	0.5	1.6	2.9	4.7	5.6	8.3	20

566

567

Nat. Hazards Earth Syst. Sci. Discuss., doi:10.5194/nhess-2017-75, 2017
Manuscript under review for journal Nat. Hazards Earth Syst. Sci.
Discussion started: 4 May 2017

Natural Hazards and Earth System Sciences
Discussions

568 Table 4. TES building capacity during the tsunami event considering the Mw 9.0 scenario.

No.	Building height	Total floor	Total evacuation area (m^2)	Evacuation area in each floor (m^2)	10^{th} percentile			50^{th} percentile			90^{th} percentile		
					Inundation depth (m)	Number of evacuation floor	Capacity during tsunami (person)	Inundation depth (m)	Number of evacuation floor	Capacity during tsunami (person)	Inundation depth (m)	Number of evacuation floor	Capacity during tsunami (person)
1	10	1	2475	2475	0	1	2475	2.9	0	0	6	0	0
2	20	5	3300	660	0.5	4	2640	3.9	3	1980	7	2	1320
3	15	3	3300	1100	0	3	3300	1.4	2	2200	4.6	1	1100
4	15	4	3300	825	0	4	3300	2.6	3	2475	5.7	2	1650
5	10	3	1815	605	0	3	1815	0.1	2	1210	3.1	1	605
6	20	4	3300	825	0	4	3300	0	4	3300	2.5	3	2475
7	15	3	3300	1100	0	3	3300	0	3	3300	1.9	2	2200
8	10	3	2310	770	0	3	2310	0.8	2	1540	3.6	1	770
9	10	3	1650	550	0	3	1650	0.2	2	1100	3	2	1100
10	10	3	4950	1650	0	3	4950	2.1	2	3300	5.1	1	1650
11	47	2	6600	3300	0	2	6600	0	2	6600	2.2	1	3300
12	15	3	2475	825	0	3	2475	0	3	2475	2.8	2	1650
13	52	13	4950	381	0	13	4950	0.8	12	4569	4	11	4188
14	15	4	8250	2063	0	4	8250	0	4	8250	3.1	2	4125
15	10	3	4950	1650	0.3	2	3300	3.6	1	1650	6.7	0	0
16	30	8	6600	825	1.2	7	5775	4.3	6	4950	7.5	5	4125
17	15	5	5280	1056	1.6	4	4224	4.8	3	3168	7.8	2	2112
18	20	4	5775	1444	0	4	5775	0.5	3	4331	3.8	2	2888
19	10	2	1650	825	0	2	1650	0	2	1650	3	1	825
20	22	5	6600	1320	1.3	4	5280	4	3	3960	6.8	2	2640
21	25	6	4950	825	0	6	4950	0.3	5	4125	2.9	5	4125
22	10	2	1650	825	0	2	1650	0.5	1	825	3.1	1	825
23	25	6	6600	1100	0.5	5	5500	2.9	5	5500	5.6	4	4400
Total capacity							**89419**			**72458**			**48073**

569

Nat. Hazards Earth Syst. Sci. Discuss., doi:10.5194/nhess-2017-75, 2017
Manuscript under review for journal Nat. Hazards Earth Syst. Sci.
Discussion started: 4 May 2017

Natural Hazards and Earth System Sciences
Discussions

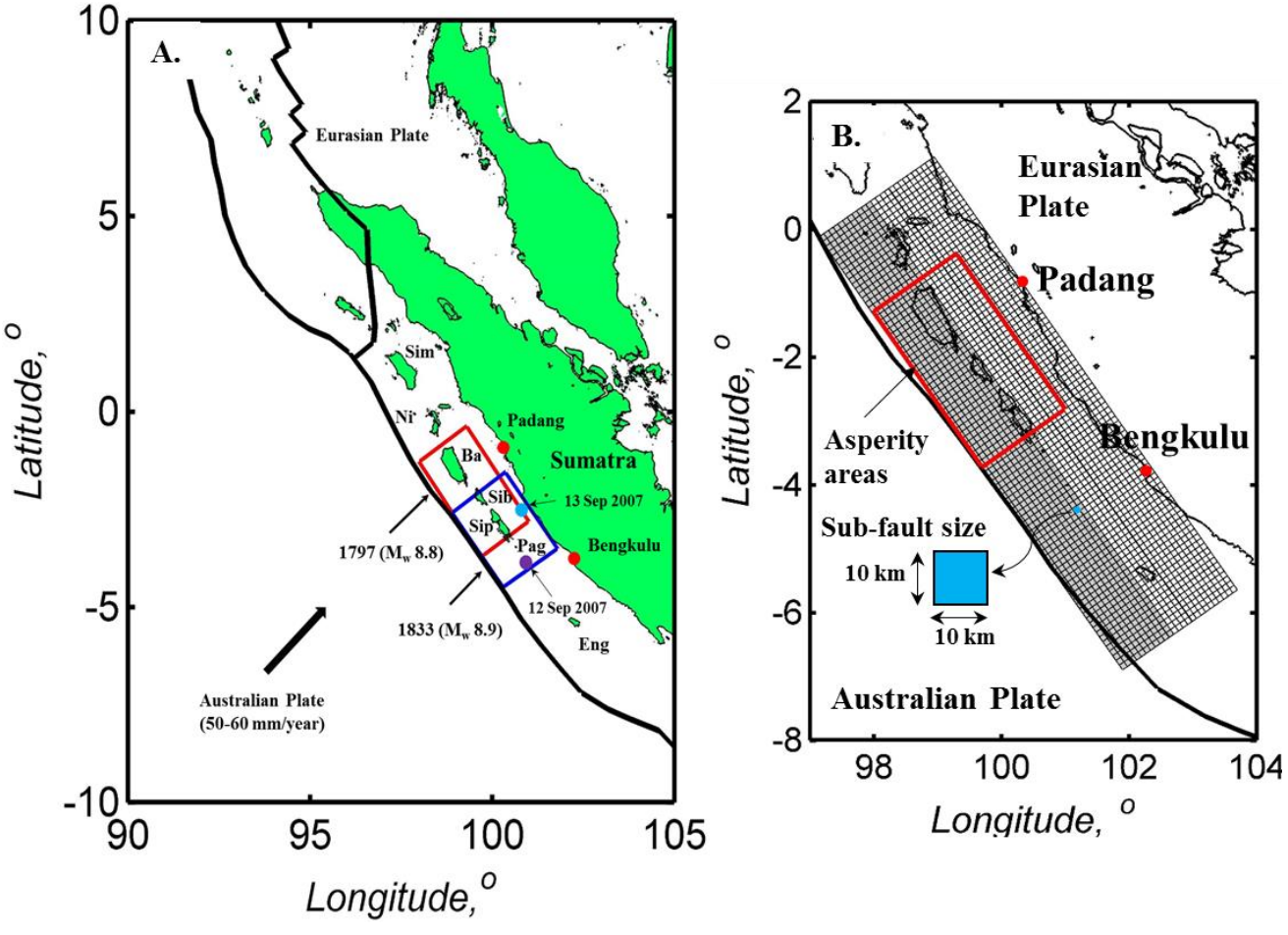

570

571 **FIGURE 1.** (A) Significant seismic events in the Mentawai segment of the Sunda subduction zone (Sim: Simeulue, Ni: Nias, Ba: Batu, Sib:
572 Sibereut, Sip: Sipora, Pag: Pagai Islands, Eng: Enggano). (B) Fault plane of the Mentawai segment source along with the asperity.
573

Nat. Hazards Earth Syst. Sci. Discuss., doi:10.5194/nhess-2017-75, 2017
Manuscript under review for journal Nat. Hazards Earth Syst. Sci.
Discussion started: 4 May 2017

Natural Hazards and Earth System Sciences
Discussions

A.

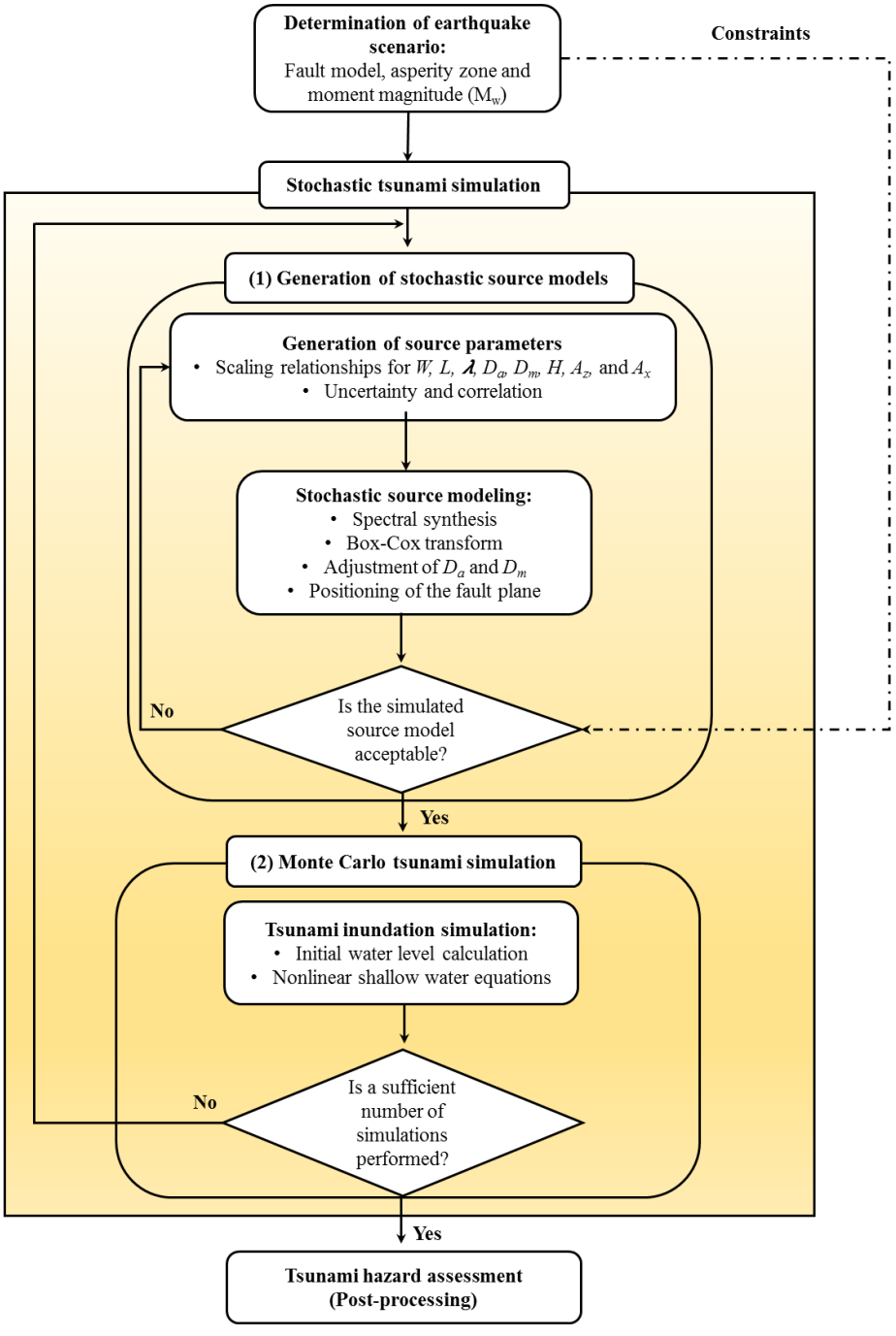

574

575 **FIGURE 2.** Procedures of stochastic tsunami simulation.

576
577

Nat. Hazards Earth Syst. Sci. Discuss., doi:10.5194/nhess-2017-75, 2017
Manuscript under review for journal Nat. Hazards Earth Syst. Sci.
Discussion started: 4 May 2017

Natural Hazards and Earth System Sciences
Discussions

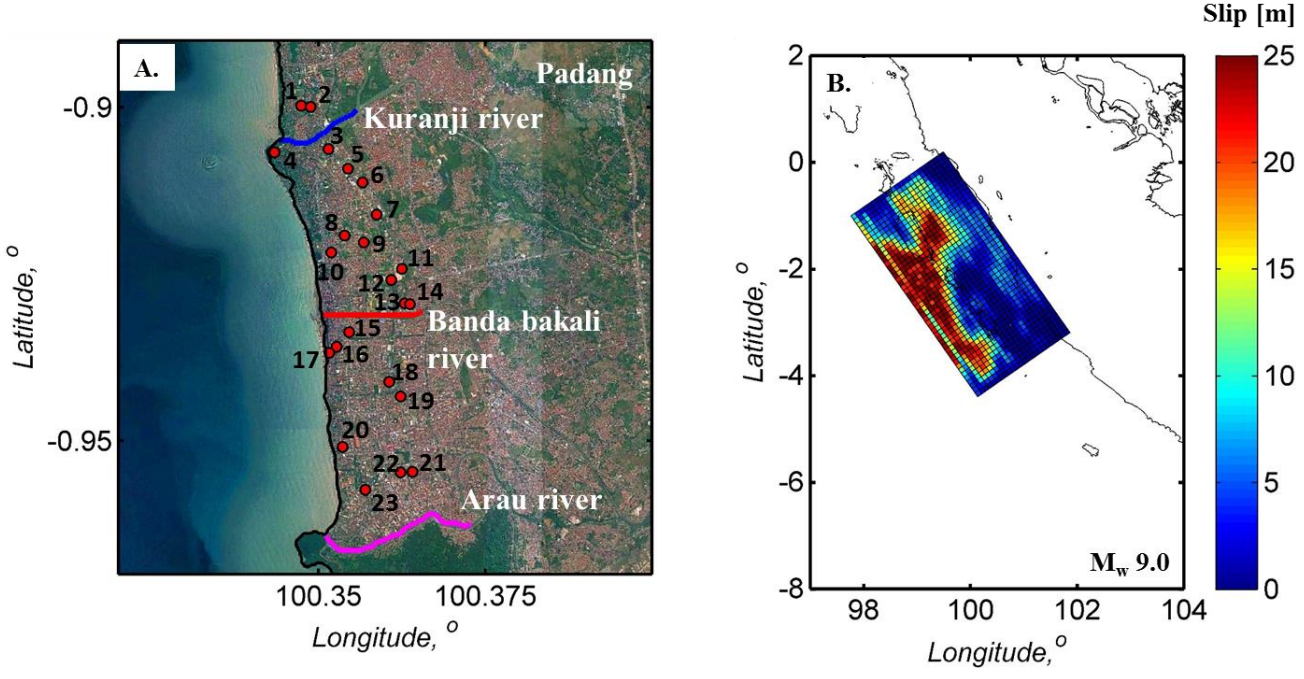

578

579 **FIGURE 3.** (A) Tsunami evacuation shelters in Padang. (B) Earthquake source models to study the effect of DEM on tsunami simulation.

580

Nat. Hazards Earth Syst. Sci. Discuss., doi:10.5194/nhess-2017-75, 2017
Manuscript under review for journal Nat. Hazards Earth Syst. Sci.
Discussion started: 4 May 2017

Natural Hazards and Earth System Sciences
Discussions

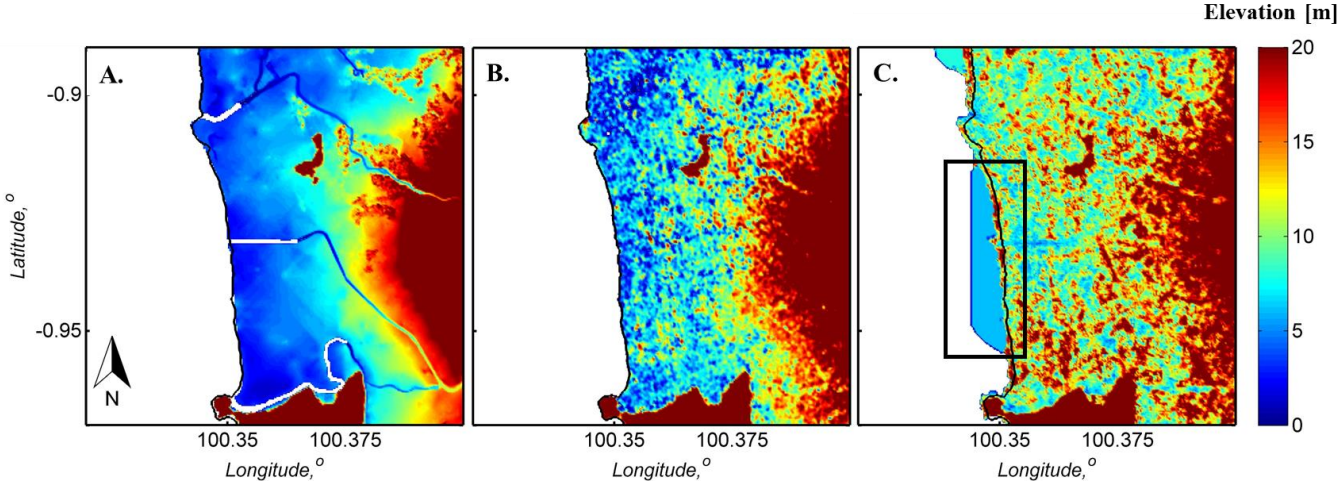

581

582 **FIGURE 4.** Digital Elevation Model for Padang: (A) DEM5. (B) SRTM1. (C) GDEM2.

583

Nat. Hazards Earth Syst. Sci. Discuss., doi:10.5194/nhess-2017-75, 2017
Manuscript under review for journal Nat. Hazards Earth Syst. Sci.
Discussion started: 4 May 2017

Natural Hazards and Earth System Sciences
Discussions

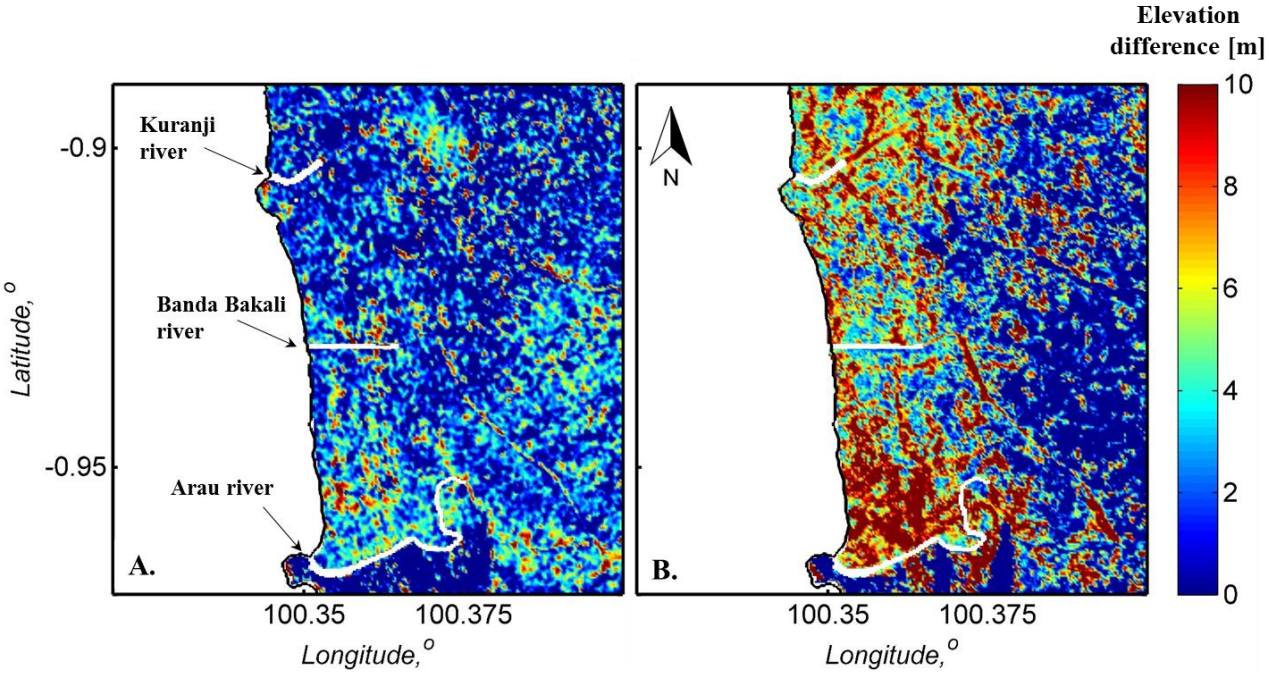

584
585 **FIGURE 5.** Elevation differences of global DEM datasets with respect to DEM5: (A) SRTM1. (B) GDEM2.
586

Nat. Hazards Earth Syst. Sci. Discuss., doi:10.5194/nhess-2017-75, 2017
Manuscript under review for journal Nat. Hazards Earth Syst. Sci.
Discussion started: 4 May 2017

Natural Hazards and Earth System Sciences
Discussions

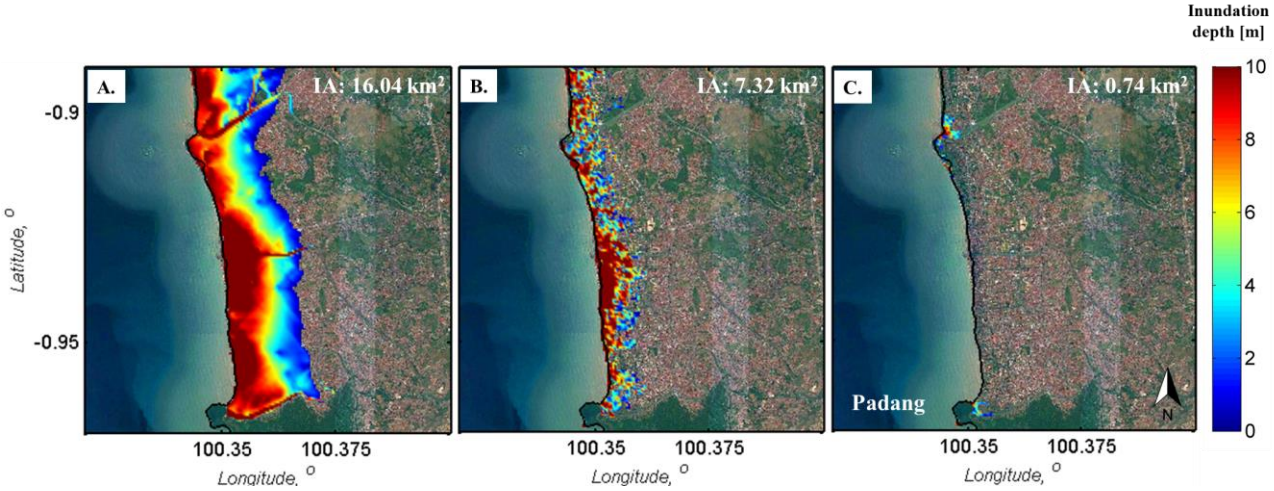

FIGURE 6. Inundation areas in Padang for: (A) DEM5. (B) SRTM1. (C) GDEM2 (IA = total inundation areas).

Nat. Hazards Earth Syst. Sci. Discuss., doi:10.5194/nhess-2017-75, 2017
Manuscript under review for journal Nat. Hazards Earth Syst. Sci.
Discussion started: 4 May 2017

Natural Hazards and Earth System Sciences
Discussions

589

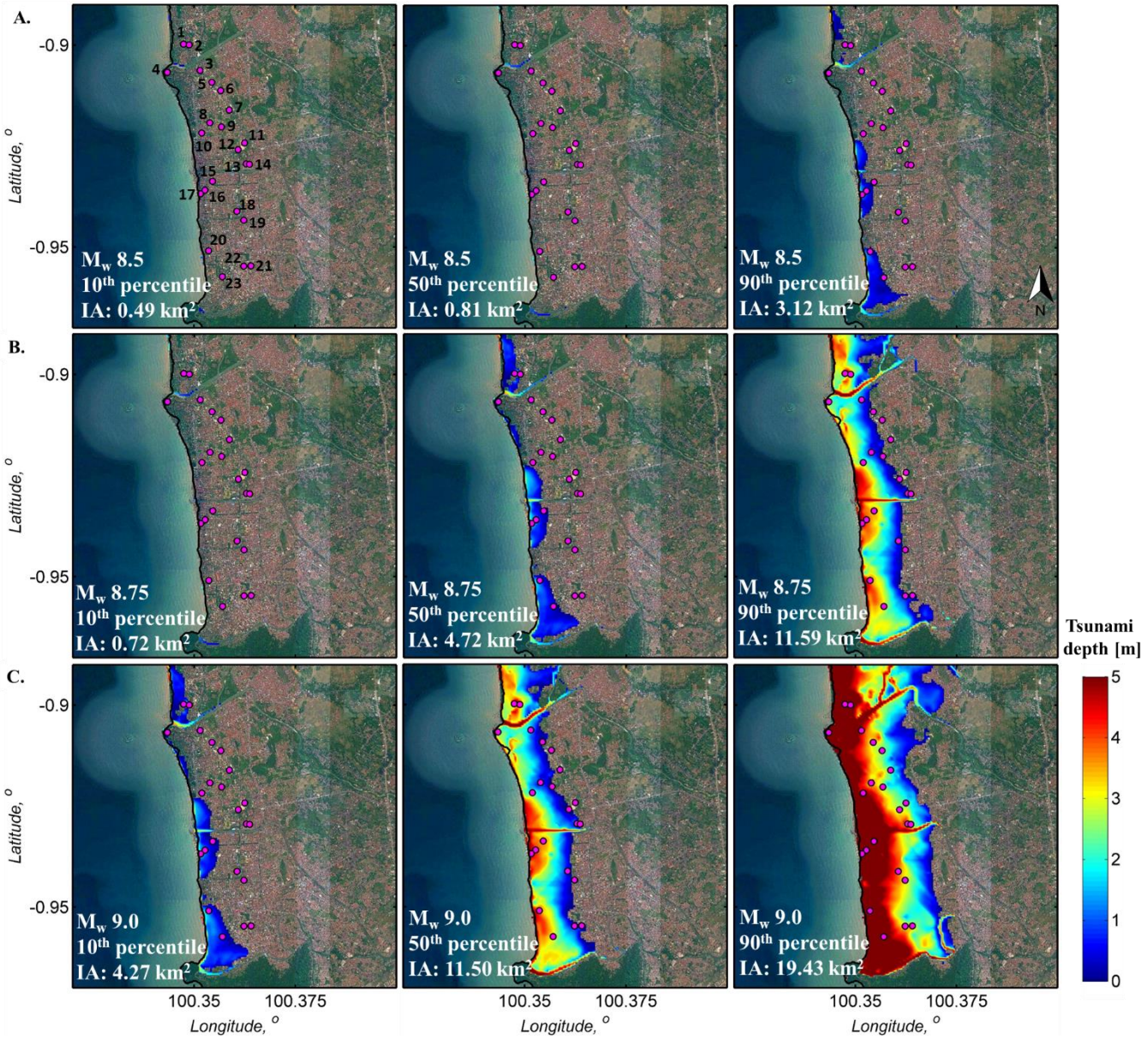

590

591 **FIGURE 7.** Inundation depth maps in Padang: (A) M_w 8.5 scenario. (B) M_w 8.75 scenario. (C) M_w 9.0 scenario (IA = inundation area).
592

Nat. Hazards Earth Syst. Sci. Discuss., doi:10.5194/nhess-2017-75, 2017
Manuscript under review for journal Nat. Hazards Earth Syst. Sci.
Discussion started: 4 May 2017

Natural Hazards and Earth System Sciences
Discussions

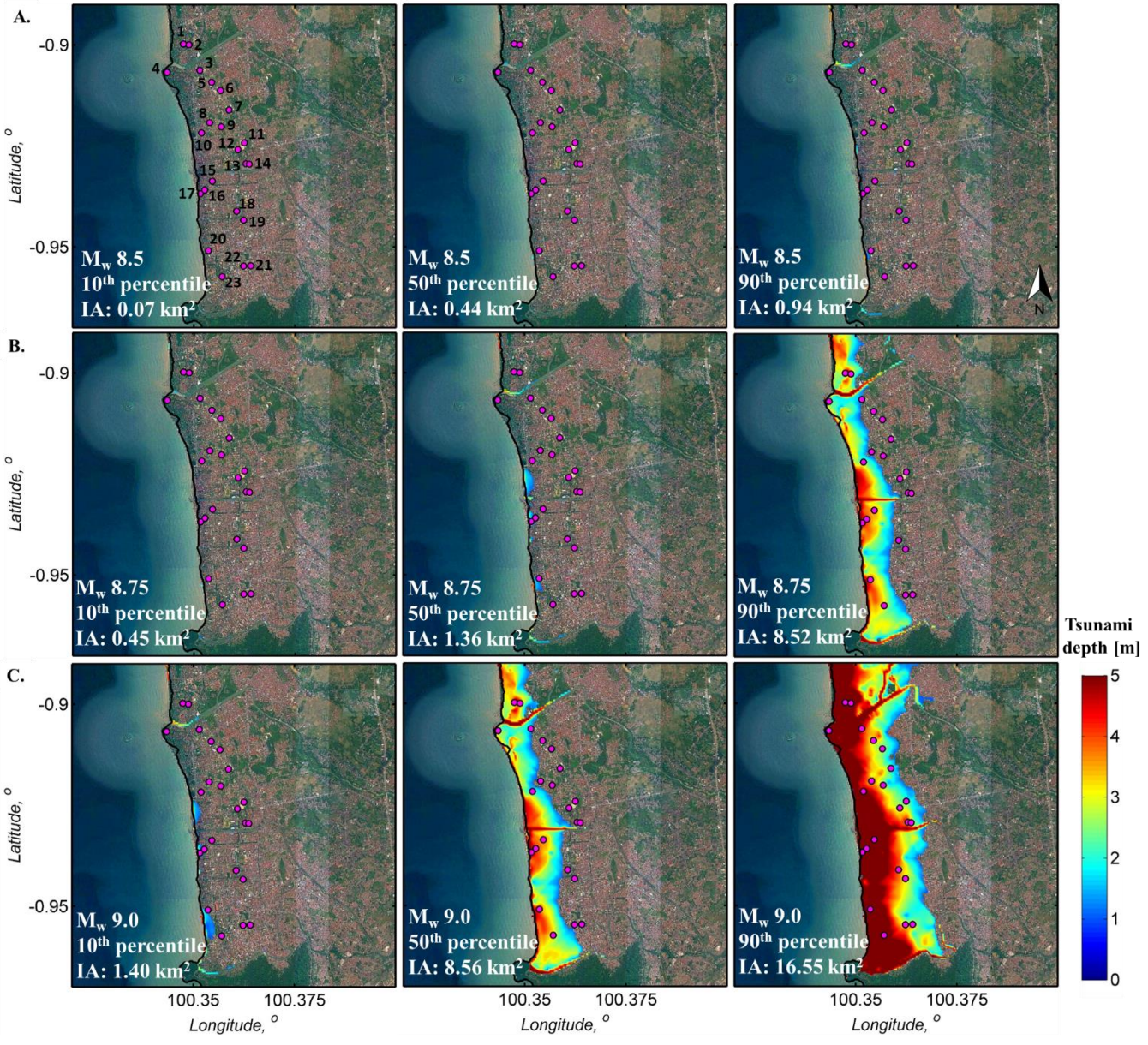

FIGURE 8. Inundation areas above 1 m depth in Padang: (A) M_w 8.5 scenario. (B) M_w 8.75 scenario. (C) M_w 9.0 scenario (IA = inundation area).

Nat. Hazards Earth Syst. Sci. Discuss., doi:10.5194/nhess-2017-75, 2017
Manuscript under review for journal Nat. Hazards Earth Syst. Sci.
Discussion started: 4 May 2017

Natural Hazards and Earth System Sciences
Discussions

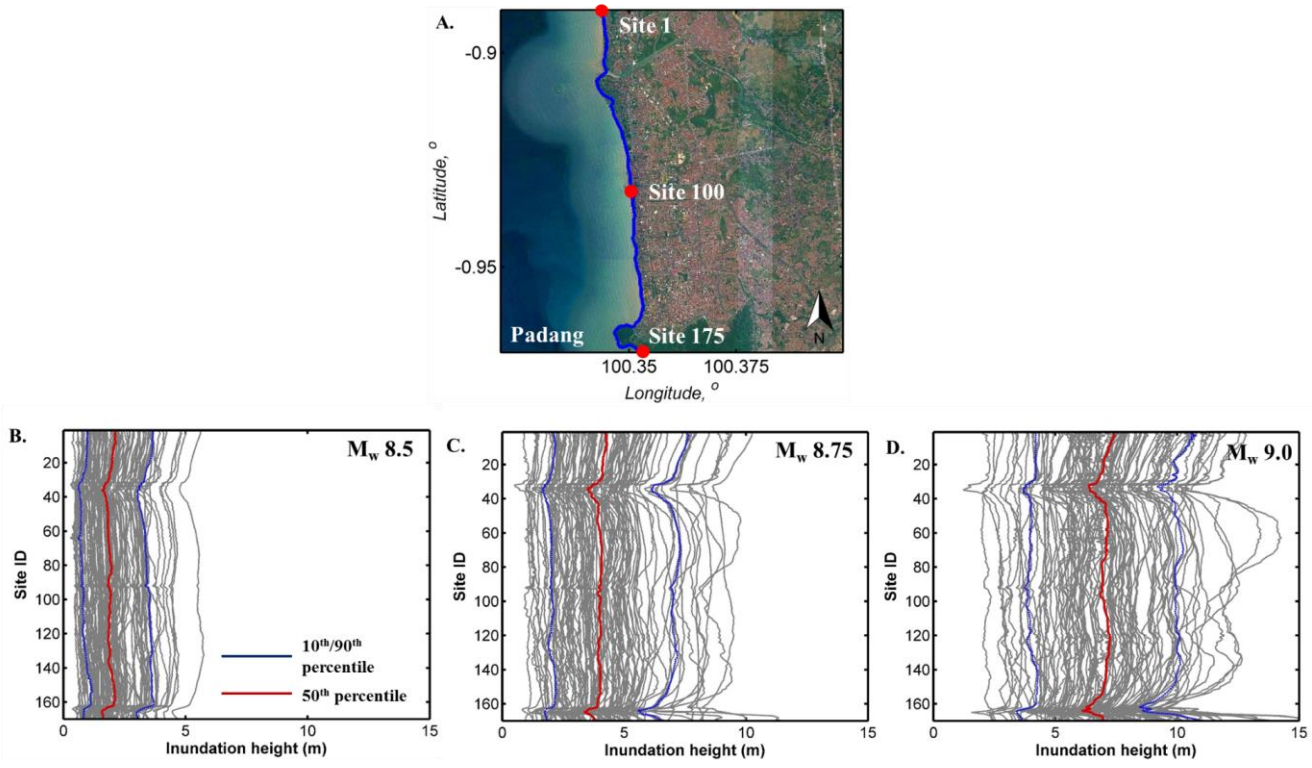

597

598 **FIGURE 9.** (A) Site location. (B) Maximum tsunami inundation height in the coastal line of Padang for the M_w 8.5 scenario. (C) Maximum
599 tsunami inundation height in the coastal line of Padang for the M_w 8.75 scenario. (D) Maximum tsunami inundation height in the coastal
600 line of Padang for the M_w 9.0 scenario.

Nat. Hazards Earth Syst. Sci. Discuss., doi:10.5194/nhess-2017-75, 2017
Manuscript under review for journal Nat. Hazards Earth Syst. Sci.
Discussion started: 4 May 2017

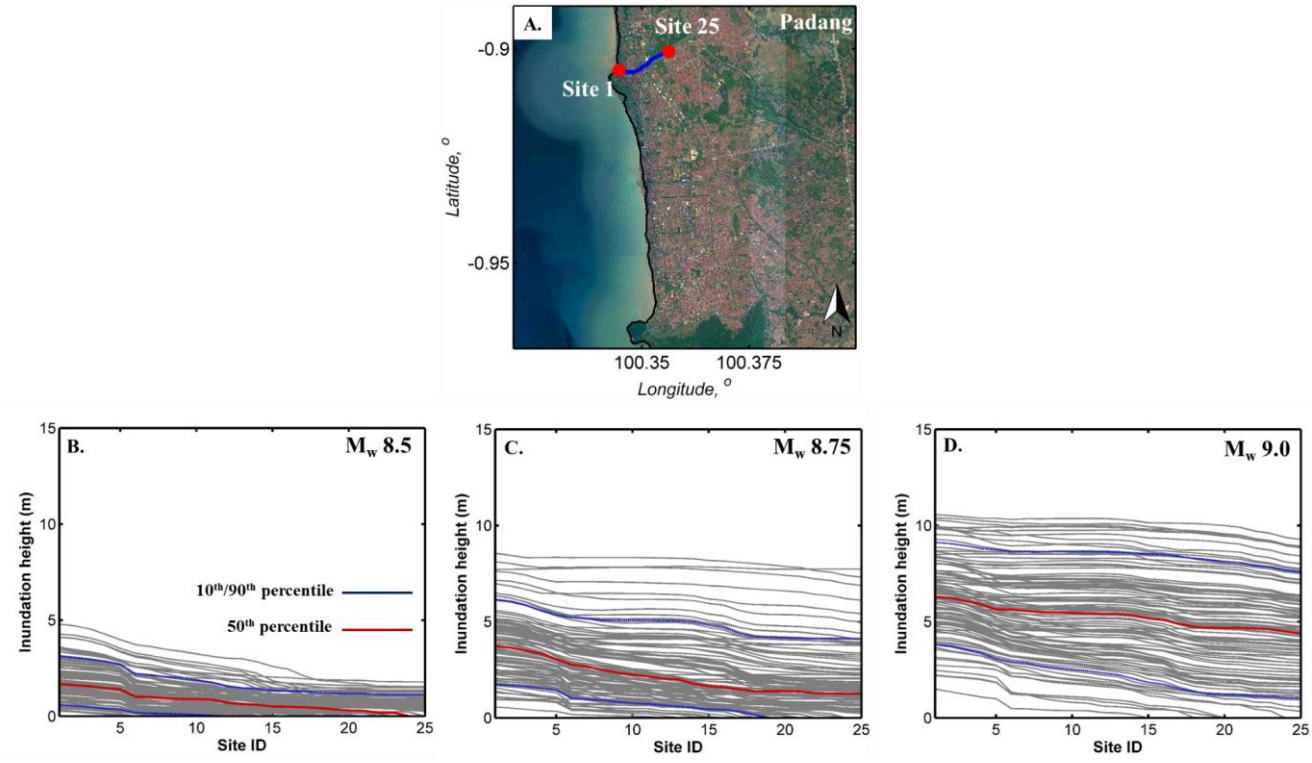

601

602 **FIGURE 10.** (A) Site location. (B) Maximum tsunami inundation height in the first river of Padang for the M_w 8.5 scenario. (C) Maximum
603 tsunami inundation height in the first river of Padang for the M_w 8.75 scenario. (D) Maximum tsunami inundation height in the first river of
604 Padang for the M_w 9.0 scenario.

Nat. Hazards Earth Syst. Sci. Discuss., doi:10.5194/nhess-2017-75, 2017
Manuscript under review for journal Nat. Hazards Earth Syst. Sci.
Discussion started: 4 May 2017

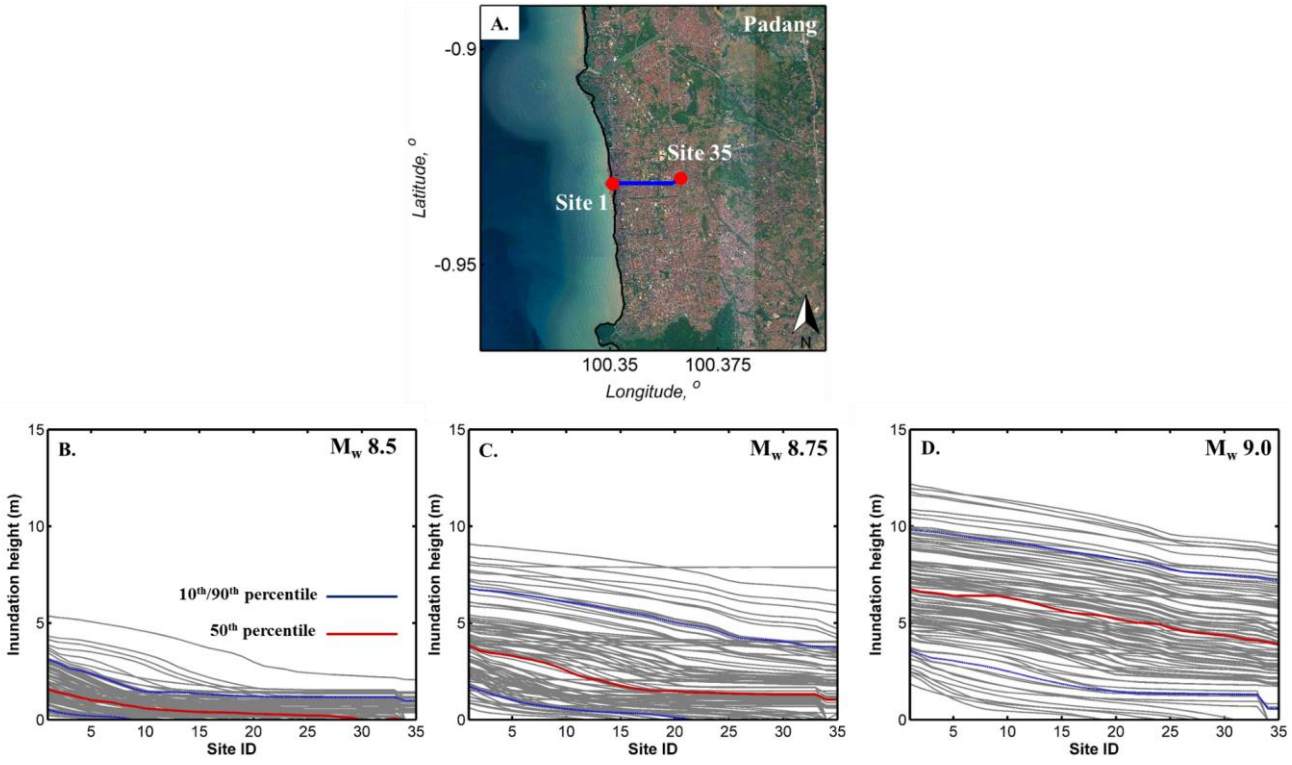

FIGURE 11. (A) Site location. (B) Maximum tsunami inundation height in the second river of Padang for the M_w 8.5 scenario. (C) Maximum tsunami inundation height in the second river of Padang for the M_w 8.75 scenario. (D) Maximum tsunami inundation height in the second river of Padang for the M_w 9.0 scenario.

Nat. Hazards Earth Syst. Sci. Discuss., doi:10.5194/nhess-2017-75, 2017
Manuscript under review for journal Nat. Hazards Earth Syst. Sci.
Discussion started: 4 May 2017

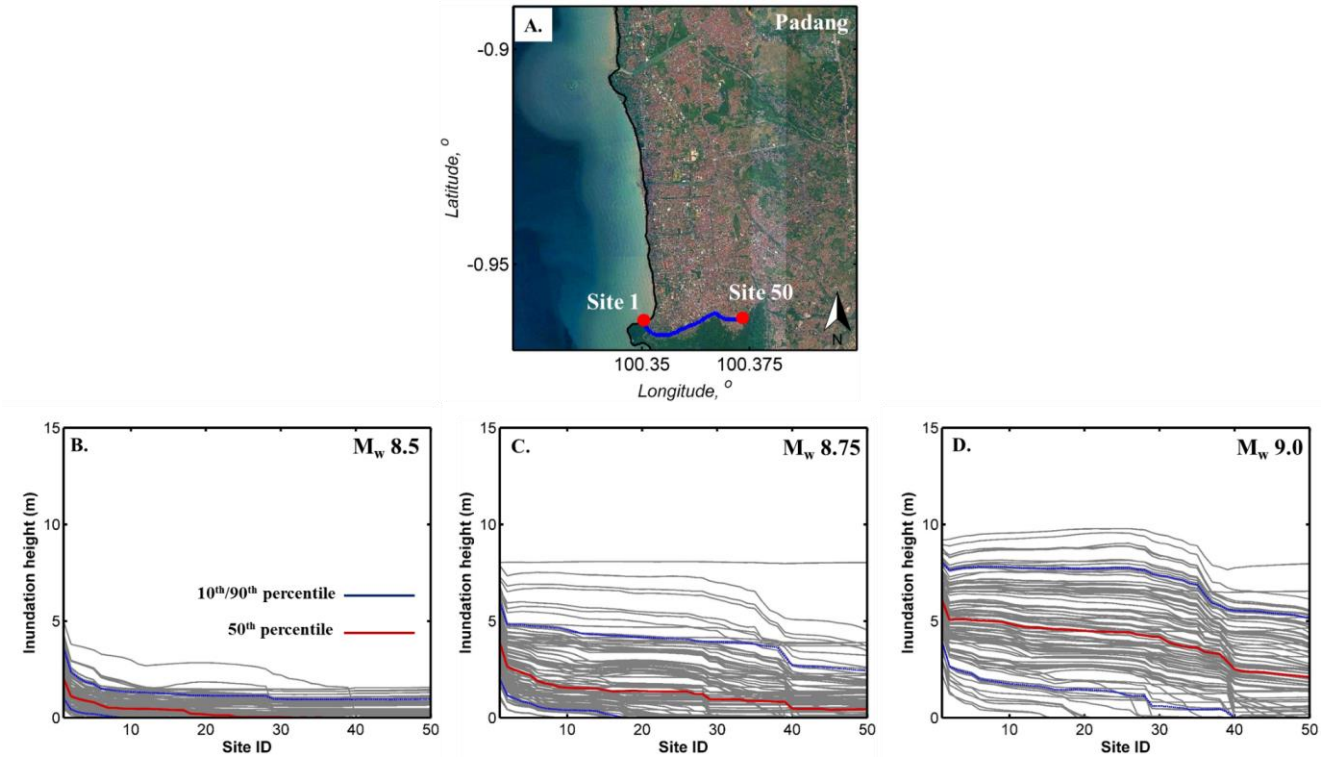

610
611 **FIGURE 12.** (A) Site location. (B) Maximum tsunami inundation height in the third river of Padang for the M_w 8.5 scenario. (C) Maximum
612 tsunami inundation height in the second river of Padang for the M_w 8.75 scenario. (D) Maximum tsunami inundation height in the third river
613 of Padang for the M_w 9.0 scenario.
614

Nat. Hazards Earth Syst. Sci. Discuss., doi:10.5194/nhess-2017-75, 2017
Manuscript under review for journal Nat. Hazards Earth Syst. Sci.
Discussion started: 4 May 2017

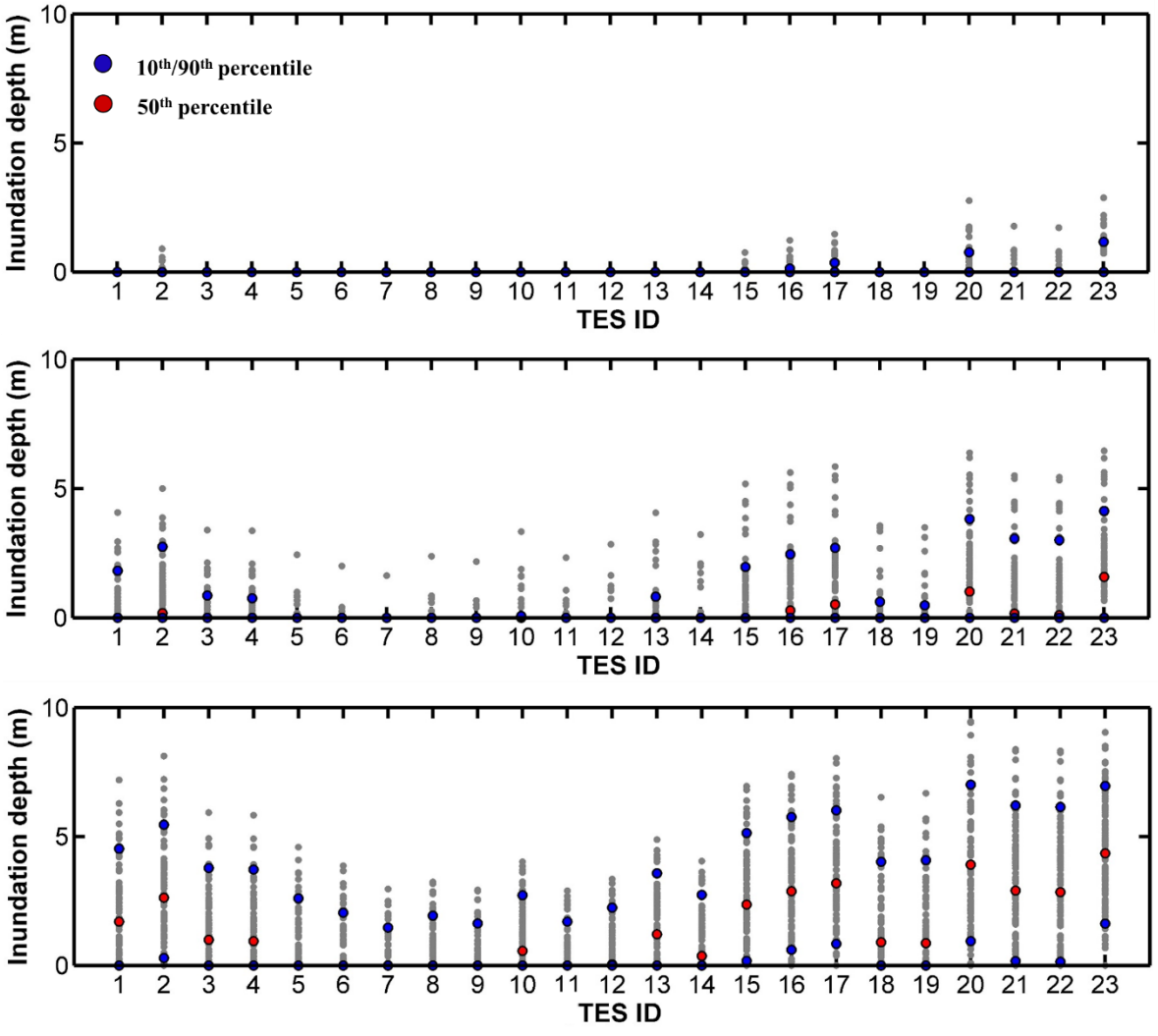

615

616 **FIGURE 13.** Inundation depth variability at TES stations for (A) M_w 8.5 scenario. (B) M_w 8.75 scenario. (C) M_w 9.0 scenario.
617

Nat. Hazards Earth Syst. Sci. Discuss., doi:10.5194/nhess-2017-75, 2017
Manuscript under review for journal Nat. Hazards Earth Syst. Sci.
Discussion started: 4 May 2017

Natural Hazards and Earth System Sciences
Discussions

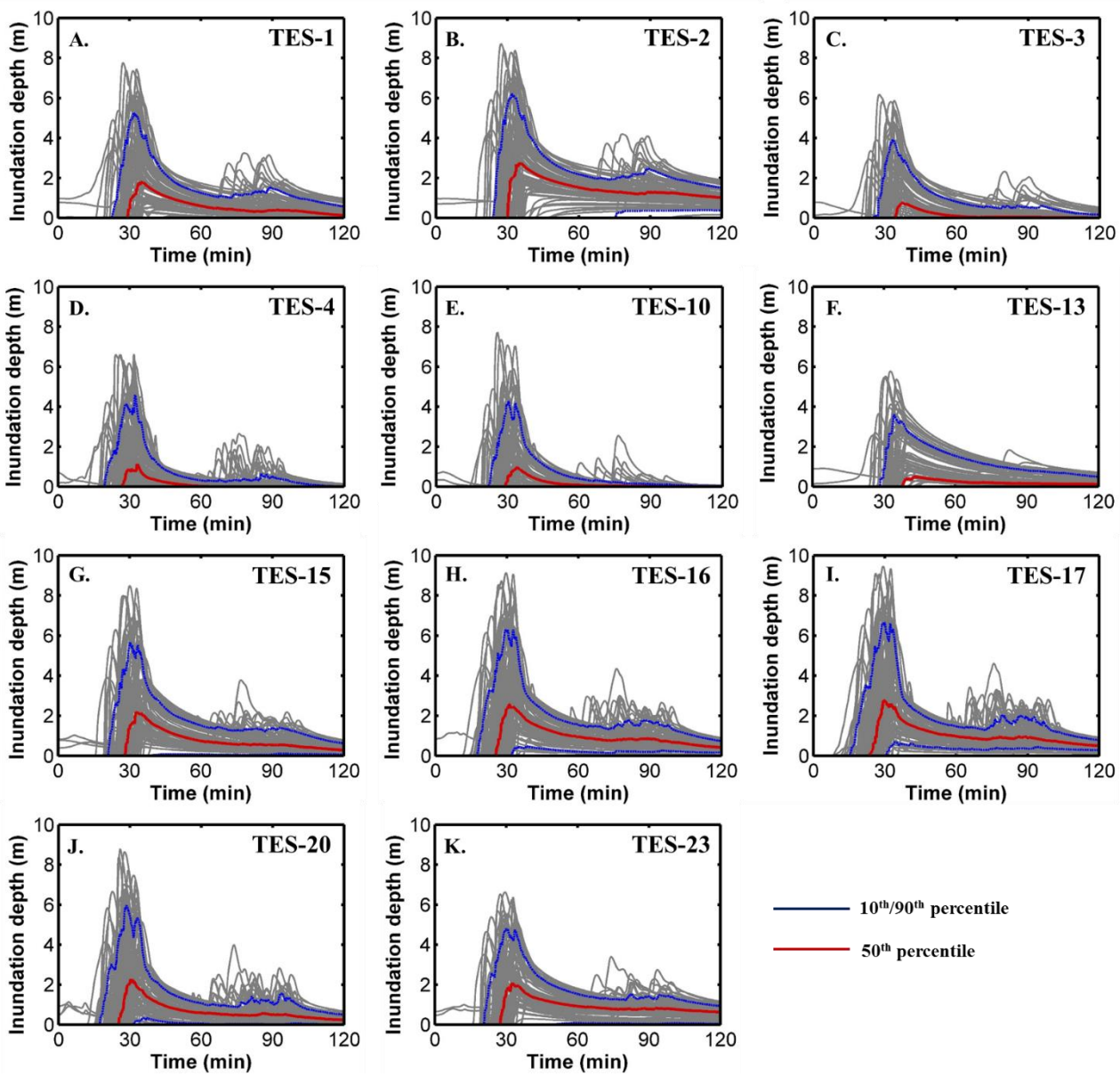

FIGURE 14. (A-K) Inundation depth variability at TES stations located near the coastal line and the rivers.

Nat. Hazards Earth Syst. Sci. Discuss., doi:10.5194/nhess-2017-75, 2017
Manuscript under review for journal Nat. Hazards Earth Syst. Sci.
Discussion started: 4 May 2017

Natural Hazards and Earth System Sciences
Discussions

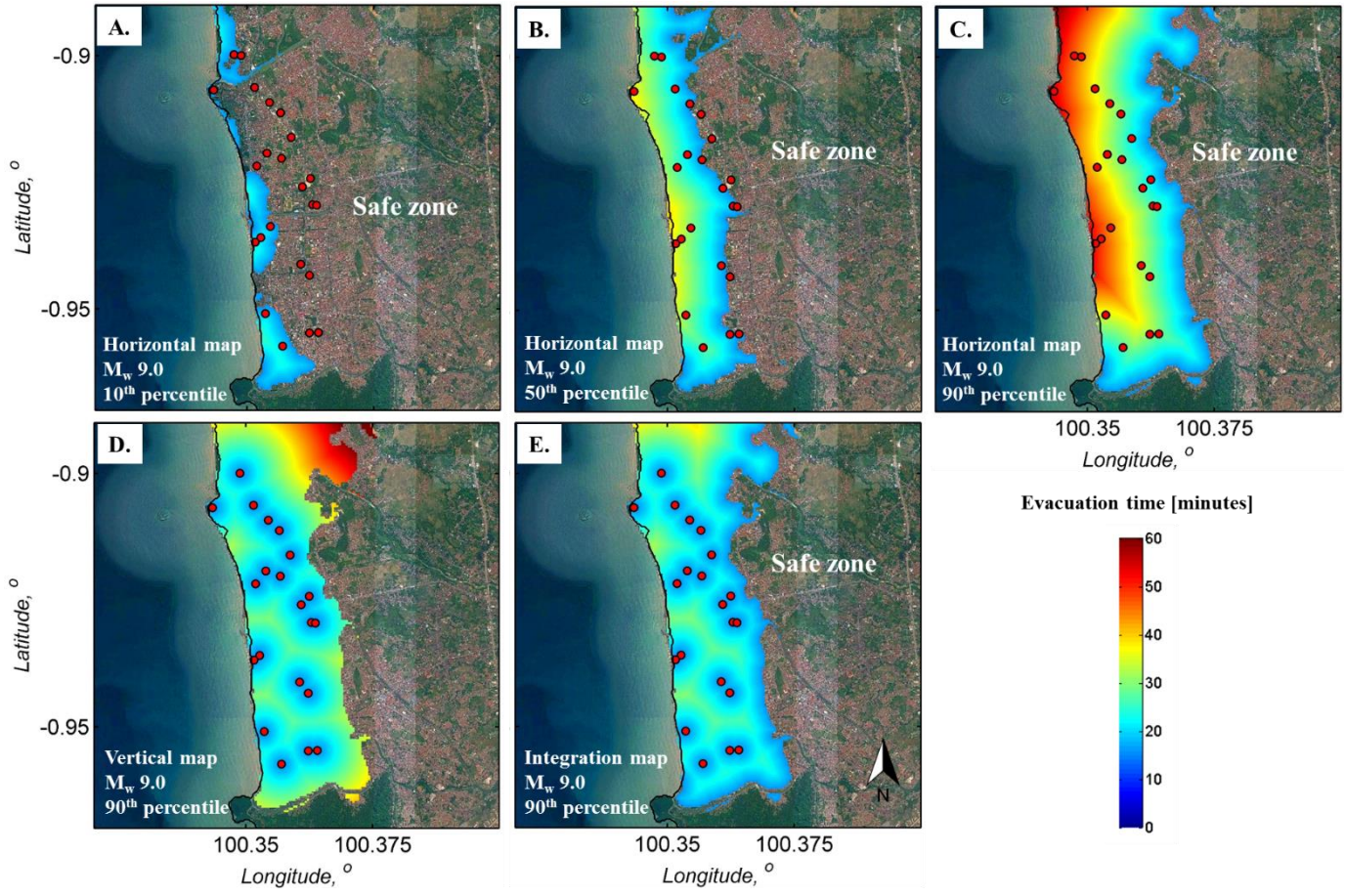

FIGURE 15. (A) Horizontal tsunami evacuation time maps in Padang for the 10th percentile. (B) Horizontal tsunami evacuation time maps in Padang for the 50th percentile. (C) Horizontal tsunami evacuation time maps in Padang for the 90th percentile. (D) Vertical tsunami evacuation time maps in Padang for the 90th percentile. (E) Integrated tsunami evacuation time maps in Padang for the 90th percentile.